β-importin Tnpo-SR promotes germline stem cell maintenance and oocyte differentiation in female *Drosophila*

Allison N. Beachum,

Taylor D. Hinnant,

Anna E. Williams,

Amanda M. Powell,

Elizabeth T. Ables[*]

Department of Biology, East Carolina University, Greenville, NC 27858.

Abstract

Germ cell development requires interplay between factors that balance cell fate and division. Early in their development, germ cells in many organisms divide mitotically with incomplete cytokinesis. Key regulatory events then lead to the specification of mature gametes, marked by the switch to a meiotic cell cycle program. Though the regulation of germ cell proliferation and meiosis are well understood, how these events are coordinated during development remains incompletely described. Originally characterized in their role as nucleo-cytoplasmic shuttling proteins, β-importins exhibit diverse functions during male and female gametogenesis. Here, we describe novel, distinct roles for the β-importin, *Transportin-Serine/Arginine rich* (*Tnpo-SR*), as a regulator of the mitosis to meiosis transition in the *Drosophila* ovary. We find that *Tnpo-SR* is necessary for germline stem cell (GSC) establishment and self-renewal, likely by controlling the response of GSCs to bone morphogenetic proteins. Depletion of *Tnpo-SR* results in germ cell counting defects and loss of oocyte identity. We show that in the absence of *Tnpo-SR*, proteins typically suppressed in germ cells when they exit mitosis fail to be down-regulated, and oocyte-specific factors fail to accumulate. Together, these findings provide new insight into the balance between germ cell division and differentiation and identify novel roles for β-importins in germ cell development.

Graphical Abstract

[*]**CORRESPONDING AUTHOR:** Elizabeth T. Ables, East Carolina University, Department of Biology, 1001 E. 10th St., Mailstop 552, 553 Science & Technology Building, Greenville, NC 27858, Office phone: 252-328-9770, ablese@ecu.edu.
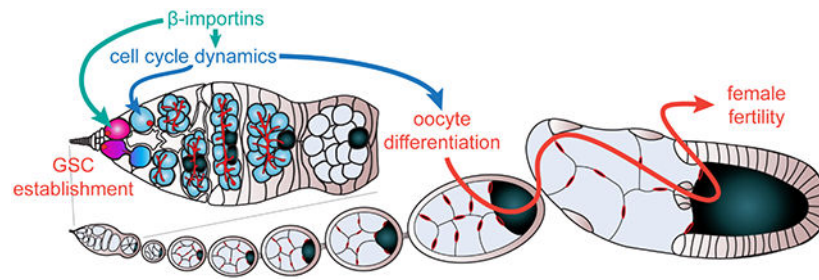
Keywords

Tnpo-SR; oogenesis; cyst; germline; germ cell

INTRODUCTION

Oocytes develop from pools of mitotically dividing undifferentiated germ cells through a series of sequential differentiation steps. In many organisms, maintenance of the undifferentiated germ cell pool relies on continuously active germline stem cell (GSC) populations to maintain gamete production (Lehmann, 2012). GSC daughter cells function as transit-amplifying populations, synchronously developing as cysts of interconnected progenitor cells (Lu et al., 2017; Matova and Cooley, 2001; Pepling and Lei, 2018). Cyst formation increases cytoplasmic volume, enhances sensitivity to DNA damage, and ensures robust oocyte development (de Cuevas et al., 1997; O'Connell and Pepling, 2021; Pepling and Lei, 2018; Yamashita, 2018). To complete differentiation, GSC daughter cells exit proliferative cell cycles and transition to the meiotic cell cycle. The molecular mechanisms that promote the switch from proliferation to differentiation must be tightly regulated to ensure tissue maintenance and oocyte production; however, these mechanisms remain incompletely described.

The fruit fly, *Drosophila melanogaster*, is an elegant model to study the molecular mechanisms that regulate the mitotic to meiotic transition. In adult females, oocytes are produced in a linear spatiotemporal arrangement fueled by the activity of GSCs (Figure 1A) (Hinnant et al., 2020). GSCs divide asymmetrically, giving rise to one daughter that remains a GSC and a cystoblast that differentiates. Delayed abscission between the GSC and cystoblast keeps the pair connected well into G2 of the subsequent cell cycle (Ables and Drummond-Barbosa, 2013; Eikenes Å et al., 2015; Hinnant et al., 2017; Mathieu et al., 2013; Matias et al., 2015). Cystoblasts divide exactly four times with incomplete cytokinesis, creating 16-cell cysts. At the completion of the mitotic divisions, cleavage furrows between germ cells are modified into stable ring canals (Grieder et al., 2000; Guertin et al., 2002; Hinnant et al., 2020). The fusome, a cytoplasmic organelle composed of microtubules, endoplasmic reticulum-derived vesicles, and membrane skeleton proteins, traverses the intercellular bridges (Hinnant et al., 2020; Ong and Tan, 2010; Pepling and Lei, 2018; Röper, 2007; Snapp et al., 2004). The fusome branches as mitotic divisions progress, providing a synchronization hub for cell cycle regulation and cell polarity, as well as a convenient marker for evaluation of germ cell differentiation (Grieder et al., 2000; Hinnant et al., 2020; Lighthouse et al., 2008; Villa-Fombuena et al., 2021). These

specialized cytological features of germ cells facilitate interconnectivity and are vital to oocyte differentiation.

Precise spatiotemporal control over cell cycle regulators underlies the transition to the oocyte fate. For example, the mitotic cyclin CycA is critical to support differentiation. Failure to degrade CycA leads to self-renewal failure in GSCs, extra mitotic divisions, and loss of oocyte identity in cyst cells (Chen et al., 2009; Ji et al., 2017; Lilly et al., 2000; Morris et al., 2005; Ohlmeyer and Schüpbach, 2003; Sugimura and Lilly, 2006). Moreover, the deubiquitinase encoded by *bag of marbles* (*bam*), one of the few known differentiation factors in *Drosophila* germ cells, is necessary and sufficient for cystoblast division and differentiation, at least in part because it stabilizes CycA expression in dividing cysts (Ji et al., 2017). Bam expression and CycA/Cdk1 activity are high in 2-cell and 4-cell cysts, but wanes as cysts approach the terminal mitotic division (Hinnant et al., 2017; Lilly et al., 2000; McKearin and Ohlstein, 1995). Since cystoblasts divide exactly four times, prior studies posited the model that cystoblasts autonomously limit the number of divisions through a molecular counting mechanism that involves Bam, CycA, and the fusome (Hinnant et al., 2020; Huynh, 2006; Ji et al., 2017; King, 1970; Lilly et al., 2000; McKearin, 1997). While a counting mechanism would limit the number of mitotic divisions, it must also promote modification of contractile ring proteins to block cytokinesis, stabilize intercellular bridges into stable ring canals, and maintain the biosynthesis of the fusome (McKearin, 1997).

We previously identified *Transportin-Serine/Arginine rich* (*Tnpo-SR;* also known as *Trn-SR*) in a genetic mosaic screen for genes controlling GSC self-renewal and germ cell development (Ables et al., 2016). *Tnpo-SR*, homologous to mammalian *TNPO3*, encodes a β-importin (Allemand et al., 2002; Kataoka et al., 1999; Kimura et al., 2021; Lai et al., 2001; Maertens et al., 2014). Like other importins, Tnpo-SR facilitates transport of cargo proteins in and out of the nucleus through nuclear pores, and is one of 16 evolutionarily conserved β-importins encoded in the *Drosophila* genome (Quan et al., 2008). β-importins are characterized by tandem huntingtin, elongation factor 3, protein phosphatase 2A and mechanistic target of rapamycin (HEAT) repeats and are generally thought to bind cargo proteins through a consensus nuclear localization or export signal (NLS or NES). Recent biochemical studies, however, demonstrate that β-importins also bind cargo proteins lacking canonical NLS/NES motifs (Kimura et al., 2021; Soniat and Chook, 2015). For example, both human TNPO3 and *Drosophila* Tnpo-SR bind to RNA recognition motifs (RRMs) and arginine/serine rich regions of Ser/Arg-rich (SR) proteins, but can also bind proteins lacking either of those domains (Kataoka et al., 1999; Kimura et al., 2017; Maertens et al., 2014). Heterogeneity in cargo binding motifs may also reflect unique biological roles for β-importins, particularly since individual β-importins appear to carry distinct sets of cargo (Kimura et al., 2017). Moreover, although many β-importins are constitutively expressed, at least some are developmentally regulated and necessary for specific developmental processes, including germ cell development, cell fate specification, cell cycle control, chromatin organization, and cell-cell communication (Hogarth et al., 2005; Kimura and Imamoto, 2014; Kimura et al., 2017; Mihalas et al., 2015; Nachury et al., 2001; Nathaniel et al., 2021). Indeed, although most β-importins have not been characterized in the context of

Drosophila germ cell development, a recent study identified specific roles for *Importin 9* in chromosome segregation during female and male meiosis (Palacios et al., 2021).

Here, we demonstrate that *Tnpo-SR* is necessary for germ cell development in *Drosophila*. We find that Tnpo-SR is expressed in female germ cells, with highest protein accumulation in GSCs and dividing cystoblasts/2-cell cysts and in endocycling nurse cells. Consistent with its expected role as a shuttling protein, Tnpo-SR is enriched intracellularly in nuclei and at the nuclear membrane, but can also be found in lower levels in germ cell cytoplasm. Mirroring Tnpo-SR expression, spatially controlled loss-of-function experiments suggest that *Tnpo-SR* predominantly acts in GSCs, cystoblasts, and the first two mitotic divisions to control germ cell development. Depletion of *Tnpo-SR* resulted in germ cell and oocyte loss, germ cell counting defects, and tumorous cysts filled with undifferentiated cells. These defects appear to arise from two main sources: depletion of GSCs and failure to exit mitotic cyst divisions into differentiated fates. We provide evidence that *Tnpo-SR*-depleted GSCs have smaller fusomes and an impaired response to bone morphogenetic signals but do not prematurely express the differentiation factor Bam. Moreover, we find that counting defects in *Tnpo-SR*-depleted germ cell cysts arise, at least in part, due to failure to adequately repress Bam, resulting in egg chambers with more than 16 germ cells, frequently lacking oocytes. Finally, we use a germline RNAi screen to identify similar roles for the Tnpo-SR paralog Cadmus (Cdm) and the GTP-binding protein Ran in GSC maintenance and cyst division. Taken together, our results support the model that that β-importins are non-redundant and regulate distinct aspects of germ cell development.

RESULTS

Tnpo-SR is expressed in the ovarian germline and exhibits variable intracellular localization.

The *Tnpo-SR* gene locus encodes two mRNA isoforms producing a single common protein. Low amounts of *Tnpo-SR* mRNA are expressed in germ cells, with the highest levels in GSCs, cystoblasts, and mitotically-dividing (2-, 4-, 8-cell) cysts (Slaidina et al., 2021). To assess Tnpo-SR protein expression in the ovary, we used CRISPR/Cas9 genome editing to insert a fluorescent tag (mCherry) endogenously at the C-terminus, creating *Tnpo-SR::mCherry* (Figure 1B–D'). We co-localized anti-mCherry antisera in whole mount immunofluorescence with antibodies against Hu li tai shao (Hts), a cytoskeletal protein that localizes to fusomes in germ cells and plasma membranes in follicle cells, and LaminC (LamC), a nuclear membrane protein that is enriched in cap cells and nurse cell nuclei. We detected low levels of Tnpo-SR::mCherry protein throughout the anterior ovariole (Figure 1B–B'). Tnpo-SR::mCherry protein was especially concentrated in nurse cell and oocyte nuclei by stage 3 of oogenesis (Figure 1C–C') and partly co-localized with LamC (see insets in Figure 1C–C'). In the germarium, *Tnpo-SR::mCherry* was concentrated in the nuclei of GSCs, cystoblasts, and 2-cell cysts (Figure 1D–D'), but was largely excluded from 8-cell and 16-cell cysts (see arrow in Figure 1D). We also detected somatic expression of *Tnpo-SR::mCherry* in posterior escort cells and follicle cells.

To further assess the intracellular localization of Tnpo-SR, we created a transgene in which the full-length *Tnpo-SR* cDNA is tagged at the N-terminus with hemagglutinin (HA) and

driven under *Upstream Activating Sequence* (*UASz*) control (DeLuca and Spradling, 2018). Using the germ cell-specific *nos-Gal4* (Van Doren et al., 1998) to drive *UAS-HA-Tnpo-SR*, we co-localized anti-HA antisera with antibodies against LamC and Hts (Figure 1E–F'). In egg chambers, HA-Tnpo-SR was localized in variable levels in germ cell nuclei, at nuclear membranes, and in the cytoplasm (Figure 1E–E'). The pattern was similar in GSCs, cystoblasts, and dividing cysts in the germarium (Figure 1F–F'). Consistent with the endogenous expression, HA-Tnpo-SR appeared in higher levels in nuclei in GSCs, though localization at the nuclear membrane could not be resolved. Taken together, these data suggest that Tnpo-SR is expressed in GSCs and their daughters, and its intracellular localization is consistent with its putative role in nucleocytoplasmic shuttling.

Tnpo-SR is necessary for GSC establishment during development and maintenance in adults.

We previously identified *Tnpo-SR* in a genetic mosaic screen of lethal transposon insertion alleles for genes controlling GSC self-renewal (Ables et al., 2016). In our original screen, germ cells harboring two copies of the lethal transposon insertion *Tnpo-SR^{KG04870}* were frequently found as single cells with abnormal fusome morphology and abnormally high levels of LamC. To more rigorously test whether *Tnpo-SR* is intrinsically required in GSCs for their maintenance, we used the *Flippase* (*FLP*)/*FLP Recognition Target* (*FRT*) genetic mosaic lineage-tracing system to conditionally inactivate *Tnpo-SR* in adult GSCs (Laws and Drummond-Barbosa, 2015; Xu and Rubin, 1993). We used previously described loss-of-function alleles of *Tnpo-SR* (*Tnpo-SR^{KG04870}* and *Tnpo-SR^{LL05552}*) carrying *FRT* sites to generate germline mutant mosaic germaria (henceforth referred to as *Tnpo-SR^{GLC}*). In germline clones that arise following *FLP/FRT*-mediated recombination, the homozygous mutant (or wildtype, in case of controls) GSC and all its progeny are visualized by the absence of the GFP marker (Figure 2A–B). GFP-negative GSC clones were generated at equivalent rates in control and mutant mosaic germaria at four days after clone induction (Figure 2E). In control (mock) mosaics, where all cells are wildtype (Figure 2A), most GFP-negative GSCs were retained in mosaic germaria (Figure 2E'), and as expected, the percentage of germaria with a GFP-negative GSC declined slightly over the course of the experiment as flies aged (Figure 2E) (Pan et al., 2007). In comparison to mock mosaic controls, *Tnpo-SR^{GLC}* females (either *Tnpo-SR^{KG04870}* or *Tnpo-SR^{LL05552}*) rapidly lost GFP- (mutant) GSCs from the niche (Figure 2B, E). By eight days after clone induction, more than 60% of *Tnpo-SR^{GLC}* germline mosaic germaria of either genotype contained GFP-negative cysts without an accompanying GFP-negative GSC (Figure 2B, E'). This "GSC loss" phenotype indicates that during the course of the assay, *Tnpo-SR* mutant GSCs produced daughter cells, but were subsequently lost from the niche. Intriguingly, we did not detect dramatic differences in GSC proliferation in *Tnpo-SR* mutant GSCs. Using antibodies against the mitotic protein phosphorylated Histone H3 (pHH3), the mitotic index of *Tnpo-SR^{GLC}* mutant GSCs (*Tnpo-SR^{LL05552}* = 5%, n = 40; *Tnpo-SR^{KG04870}* = 5%, n = 20) was not statistically different from wild-type GSCs (*FRT40A* control = 6%, n = 94).

To further investigate the role of *Tnpo-SR* in GSCs and their daughters, we generated a germline-enhanced short hairpin interfering RNA (RNAi) transgene (using the *VALIUM22* targeting vector) (Ni et al., 2011) targeting exon five of *Tnpo-SR*. The *Tnpo-SR^{RNAi}* is

highly efficient at depleting HA-Tnpo-SR from germ cells (Supplementary Figure S1). We then used the germline-specific *nos-Gal4* to induce *Tnpo-SR* knockdown in germ cells at their earliest stages of development and counted the number of GSCs per germarium in adult females over four timepoints in the first 10 days after eclosion (Figure 2C–D, F). Ovaries were immunostained for Hts and LamC, and GSCs were identified by their anteriorly localized fusome juxtaposed to cap cells (de Cuevas and Spradling, 1998; Lin et al., 1994). *Tnpo-SR^{RNAi}* germaria had fewer GSCs than driver-only controls at eclosion; moreover, the number of *Tnpo-SR^{RNAi}* GSCs continued to decline as the flies aged, in contrast to controls (Figure 2F). Taken together with the mosaic analyses of *Tnpo-SR^{GLC}* null mutants, these data indicate that *Tnpo-SR* is intrinsically necessary for GSC establishment during development, and for GSC self-renewal in adults.

Tnpo-SR mutant GSCs have smaller fusomes and are less responsive to BMP signals.

To begin to determine how *Tnpo-SR* promotes GSC self-renewal, we first considered the possibility that loss of *Tnpo-SR* might alter the adhesion of GSCs to the niche. However, levels of the adhesion protein E-cadherin, which is essential for the adhesion of GSCs to cap cells (Song et al., 2002), were equivalent between *TnpoSR^{GLC}* mutant and adjacent wild-type GSCs (Figure 2G–G', J). In the process of these analyses, we noticed that the fusome was underdeveloped in *TnpoSR^{GLC}* mutant GSCs (Figure 2G–G'). The fusome is remodeled at each GSC division: at mitosis, a small plug of fusome material is deposited at the ring canal between the GSC and the nascent cystoblast (de Cuevas and Spradling, 1998; Deng and Lin, 1997; Villa-Fombuena et al., 2021). Fusome material from the GSC/cystoblast interface then extends anteriorly to fuse with the original GSC fusome. In *Tnpo-SR^{GLC}* mutant (Figure 2G–G') or *Tnpo-SR^{RNAi}* (Figure 2I) GSCs, the Hts-positive fusome area was significantly smaller than in wild-type GSCs (Figure 2H), regardless of the stage of fusome remodeling (Figure 2K–L). We speculate that abnormal fusome morphogenesis may contribute to the failure of *Tnpo-SR*-depleted GSCs to maintain self-renewal.

We then asked whether premature differentiation might explain the loss of *Tnpo-SR* mutant GSCs. Bone morphogenetic proteins (BMPs) secreted from cap cells are necessary for GSC maintenance (Chen and McKearin, 2003; Xie and Spradling, 1998). In GSCs, reception of BMP signals by BMP receptors causes transcriptional activation of the GSC-enriched *Daughters against dpp* (*Dad*) and repression of the differentiation factor *bam* (Chen and McKearin, 2003; Song et al., 2004). To test the ability of *Tnpo-SR*-depleted GSCs to respond to BMP signals, we measured the levels of *Dad-lacZ*, a well-established reporter of BMP pathway activation (Kai and Spradling, 2003; Song et al., 2004). *Tnpo-SR^{RNAi}* GSCs had significantly lower *Dad-lacZ* fluorescence intensity than wild-type GSCs (Figure 2M–O). These data indicate that *Tnpo-SR*-depleted GSCs are unable to respond properly to BMP signals.

Depletion of Tnpo-SR alters the number of germ cells per egg chamber.

Outside of GSC loss, depletion of *Tnpo-SR* using RNAi produced additional germline phenotypes. In wild-type germaria, cystoblasts divide exactly four times with incomplete cytokinesis and the resulting cysts are encapsulated by a monolayer of follicle cells, producing egg chambers with 16 germ cells (Figure 3A, D–F) (Hinnant et al., 2020). In

contrast, RNAi knock-down of *Tnpo-SR* produced egg chambers with variable number of germ cells, both greater than and less than 16 (Figure 3B–F). Most egg chambers with 32 or more cells had oocytes with five ring canals, suggesting that some abnormal egg chambers arose by an extra mitotic division. Other egg chambers (with less than 16 cells) housed germ cells on the order of 2^n, suggesting that some cystoblasts failed to divide the requisite four times. Many egg chambers, however, deviated from the 2^n pattern (Figure 3F). This suggests that the abnormal number of germ cells is not solely due to cystoblast division errors. Moreover, germ cell numbers in adjacent chambers in *Tnpo-SR^{RNAi}* egg chambers did not always add up to 8, 16, or 32 cells. We also observed *Tnpo-SR^{RNAi}* ovarioles that contained cystic germline tumors, in which a normal follicle cell monolayer surrounded mitotically-active germ cells with short or unbranched fusomes (Figure 3C, E; Figure 4A). Tumorous egg chambers were predominately filled with single and 2-cell germ cells (as indicated by the morphology of their fusomes). Intriguingly, knock-down of *Tnpo-SR* in more differentiated 8- and early 16-cell cysts using the *bam-Gal4* driver or a *3xbam-Gal4* driver harboring three independent insertions of *bam-Gal4* (Clémot et al., 2018) (Supplementary Figure S1) did not alter the number of germ cells per egg chamber (Figure 3F). These data suggest that *Tnpo-SR* is necessary in GSCs and early germline cysts but may be dispensable at later stages of germ cell development..

Interestingly, we did not consistently observe egg chambers with more than 16 germ cells in *Tnpo-SR^{GLC}* mutants. Instead, we found *Tnpo-SR^{GLC}* germline mutant egg chambers (surrounded by wild-type follicle cells) devoid of fusomes, but still containing at least one germ cell in active mitosis (*TnpoSR^{KG}* = 16% of mutant egg chambers, n = 25; *Tnpo-SR^{LL}* = 28% of mutant egg chambers, n = 14) (Figure 4B). Since wild-type germ cells in egg chambers never express pHH3 (*FRT40A* mock mosaics = 0%, n = 52), these data indicate that loss of *Tnpo-SR* prolongs the number of mitotic divisions of cystoblasts/cysts. We also found egg chambers in which *Tnpo-SR^{GLC}* GFP-negative germ cells were encapsulated together with wild-type GFP-positive germ cells (Figure 4C).

Intriguingly, many *TnpoSR^{GLC}* mutant germ cells were recovered as single cells, frequently as small clusters in the middle to posterior third of mosaic germaria (Figure 4D). This suggested that some germ cell counting defects in *Tnpo-SR^{GLC}* mutant and *Tnpo-SR^{RNAi}* knock-down egg chambers could also arise as a result of cyst fragmentation. In support of this idea, we observed mosaic germaria in which *Tnpo-SR^{GLC}* mutant cells with thin, stretched fusomes were adjacent to one another, with fusomes aligned along the same plane as if they were connected (Figure 4E). Immunostaining with anti-pTyr antibodies to visualize ring canals highlighted *Tnpo-SR^{GLC}* mutant cysts where ring canal components accumulated on adjacent cyst cells, separated by a very thin line of GFP-positive cytoplasm (Figure 4F), indicating that cells have physically separated from each other after clone induction.

To better understand how cyst fragmentation might arise, we tested whether depletion of *Tnpo-SR* altered the protein components of the fusome in dividing cysts. Scribble (Scrib) is a scaffolding protein that localizes at the cell cortex and in immature fusomes of wild-type GSCs and dividing cysts, as visualized with a *Scrib::GFP* protein trap (Figure 4G) (Lighthouse et al., 2008). By the third mitotic division, *Scrib::GFP* is largely absent from

wild-type fusomes and does not co-localize with Hts in 16-cell cysts (circled in yellow, Figure 4G). In *Tnpo-SR*^{*RNAi*} germ cells, *Scrib::GFP* was prominently expressed in the long, thin fusomes of germ cells in the posterior of germaria (Figure 4H). Considering the *Tnpo-SR*^{*GLC*} data, we propose that continued mitotic divisions of *Tnpo-SR*-depleted germ cells weaken intracellular bridges between cyst cells, causing cysts to break apart (Figure 4I). In the RNAi model, this appears to result in incorrect separation of germ cells into egg chambers (Figure 3F) or tumor formation (Figure 3C), whereas in the clonal model (where wild-type cells are also present), germ cells are more likely to be encapsulated as singlets or doublets (as in Figure 4F).

Tnpo-SR depletion suppresses the mitotic to meiotic transition.

We then asked whether *Tnpo-SR*-depleted germ cells expressed proteins that normally accumulate in oocytes as germ cells exit the mitotic phase. In wild-type egg chambers (posterior to the germarium), the oocyte-specific protein Orb was clearly present in one posterior cyst cell (Figure 5A, C). In contrast, many egg chambers from *nos-Gal4>Tnpo-SR*^{*RNAi*} females did not contain an Orb-positive cell (Figure 5B–C). Importantly, many *Tnpo-SR*^{*RNAi*} egg chambers contained less than 16 germ cells (see Figure 3F) and as expected, the majority of these egg chambers did not contain an Orb-positive oocyte. Independent of the counting defects, however, we found evidence that loss of *Tnpo-SR* directly impacted oocyte differentiation: 34% of *Tnpo-SR*^{*RNAi*} egg chambers with 16 germ cells contained only nurse cells (Figure 5B–C). Similarly, in *Tnpo-SR*^{*GLC*} mutant mosaic germaria, most mutant cysts located posterior to wild-type cysts (thus at a more advanced stage of development) failed to up-regulate Orb expression to levels equivalent to adjacent wild-type cysts (Figure 5D–E). Further, C(3)G, a core component of the synaptonemal complex normally present as early as the 4-cell cyst stage (Hughes et al., 2018), did not accumulate in a large proportion of *Tnpo-SR*^{*GLC*} mutant cysts (Figure 5F–G). Since entry into meiosis is apparently abrogated in the absence of *Tnpo-SR*, we conclude that *Tnpo-SR* is necessary for the proper timing of oocyte differentiation.

Tnpo-SR promotes the mitotic to meiotic transition by suppressing Bam in dividing cysts.

The differentiation factor Bam is a key regulator of developmental transitions and cyst divisions (Chen and McKearin, 2003; Ji et al., 2017; McKearin and Ohlstein, 1995; Song et al., 2004). BMP signals from cap cells ensure robust transcriptional silencing of Bam in GSCs, while expression of Bam in cyst cells stabilizes the mitotic cyclin CycA in cysts to promote their division. Given that loss of *Tnpo-SR* resulted in decreased BMP responsiveness in GSCs and extra mitotic divisions in cystocytes, we explored whether these seemingly unrelated phenotypes might both arise due to mis-expression of Bam. We first asked whether the failure of *Tnpo-SR*-depleted GSCs to respond to BMP signals prematurely induced Bam expression, which could promote differentiation of the GSCs. We monitored Bam protein expression using a transgene (*Bam-sfGFP*) carrying a fosmid genomic fragment wherein *bam* was fused at the C-terminus with green fluorescent protein (GFP) (Sarov et al., 2016). Similar to previous reports describing Bam protein expression (McKearin and Ohlstein, 1995), Bam-sfGFP is absent from GSCs, highly expressed in 4-cell cysts, and weakly expressed in 2-cell and 8-cell cysts in wild-type germaria (Figure 6A, C). Similarly, Bam-sfGFP was undetectable in GSCs in *Tnpo-SR*^{*RNAi*} germaria (Figure

6D), suggesting that loss of *Tnpo-SR* is not sufficient to fully de-repress *bam* expression. Moreover, *Tnpo-SR^{RNAi}* germ cells from tumorous egg chambers also did not express Bam-sfGFP, suggesting that these germ cells have not fully differentiated (see arrows in Figure 6B).

Bam-sfGFP levels normally decrease at the 8-cell cyst stage, such that protein is not detectable in 16-cell cysts (outlined in yellow; Figure 6C, E). When we depleted *Tnpo-SR* using *nos-Gal4>Tnpo-SR^{RNAi}*, we frequently observed Bam-sfGFP expression in 16-cell cysts, suggesting that Bam expression is not adequately suppressed in 8-cell cysts (Figure 6D–E). Given that Bam regulates CycA expression (Ji et al., 2017; Liu et al., 2017), we conclude that the failure to suppress Bam, at least in part, underlies the ability of *Tnpo-SR*-depleted cells to continue to divide.

An importin RNAi screen suggests that Tnpo-SR, Cdm, and Ran may have overlapping functions during germ cell development.

Nucleo-cytoplasmic transport is essential for cellular function, and β-importins act as molecular shuttles to move proteins between the nucleus and cytoplasm (Kimura and Imamoto, 2014; Mason and Goldfarb, 2009; Nguyen and Robinson, 2020). β-importins are particularly important during mitosis, where they partner with the small guanosine triphosphate (GTP)-binding protein Ran to move protein cargo into the nucleus and promote mitotic spindle assembly (Cautain et al., 2015; Okada et al., 2008; Ozugergin and Piekny, 2020; Sazer and Dasso, 2000). To determine whether *Tnpo-SR* loss-of-function phenotypes reflect a general role for β-importins in germ cell mitoses, we performed a secondary reverse genetic screen using available germline-enhanced RNAi transgenes to knock-down expression of eight *Drosophila* importins and *Ran* specifically in germ cells (Figure 7A–D). Ovarioles were labeled with DAPI to visualize nuclei and quantified for the presence of germ cells based on the unique nuclear morphology of nurse cells and oocytes (Figure 7A–C). Most of the RNAi lines produced normal, robust ovarioles with seven to eight developing egg chambers, similar to driver-only controls (Figure 7A, D). In contrast, three of the RNAi lines produced completely agametic ovaries, defined by the complete absence of egg chambers in an ovariole (Figure 7B, D). RNAi line *Tnpo/CG8219^{RNAi}* carries a short hairpin that recognizes both *Tnpo* and the related but uncharacterized paralog *CG8219*. Since the RNAi line specific for *Tnpo* did not display germ cell phenotypes, we speculate that *Tnpo* and *CG8219* may be able to compensate for each other, as they share 80% amino acid similarity. Only one RNAi line for the β-importin *moleskin* (*msk^{RNAi-3}*) displayed an agametic phenotype, making it difficult to conclude whether the RNAi accurately reflects a role in germ cell development. Most intriguingly, three RNAi lines corresponding to *Ran* and the β-importins *cadmus* (*cdm*) and *Fs(2)Ket* (also called *Ketel*) exhibited a partial agametic phenotype similar to *Tnpo-SR^{RNAi}* (Figure 7C–D). Some ovarioles lacked germ cells completely, while other ovarioles contained germ cells, but harbored unusual egg chamber morphology (Figure 7C). Cdm and Tnpo-SR are paralogs, sharing 42% amino acid similarity, while Ketel is less conserved.

Since GSCs give rise to all germ cells, we hypothesized that agametic ovaries resulting from *Ran*, *cdm*, and *Fs(2)Ket* knock-down could arise from a failure to establish or maintain

GSCs, similar to *Tnpo-SR^RNAi*. To test this, we collected ovaries at four timepoints over the first 10 days after eclosion and quantified the number of GSCs per germarium by immunolabeling of Hts and LamC. RNAi lines targeting *cdm*, *Fs(2)Ket*, and *Ran* produced ovaries with fewer GSCs per germarium than driver-only controls at eclosion, indicating that these genes are necessary for GSC establishment (Figure 7E). Intriguingly, germaria from *nos-Gal4>cdm^RNAi* or *Ran^RNAi* showed continued GSC loss over time, suggesting that, like Tnpo-SR, these factors are necessary for GSC self-renewal. This was not the case for *Fs(2)Ket^RNAi*, however, suggesting that Fs(2)Ket does not share overlapping functions in GSCs with *Tnpo-SR*.

Expression of *cdm^RNAi* or *Ran^RNAi*, but not *Fs(2)Ket^RNAi*, in germ cells also altered the number of germ cells per egg chamber (Figure 7F). In the rare instances where control or *Fs(2)Ket* RNAi egg chambers had an abnormal number of germ cells, they invariably contained 32 cells, suggesting an extra mitotic division (Figure 7F). Like knock-down of *Tnpo-SR*, *nos-Gal4>cdm^RNAi* or *Ran^RNAi* also produced variable numbers of germ cells that did not always equal 2^n. Moreover, these phenotypes were not observed when *cdm^RNAi* or *Ran^RNAi* were driven in dividing cysts using *bam-Gal4* (Figure 7G). Taken together, these results suggest that β-importins play unique roles in the control of germ cell development, and that Tnpo-SR, cdm, and Ran may function together to regulate GSC establishment, self-renewal, and the mitotic-meiotic transition.

DISCUSSION

Our data demonstrates that the β-importin *Tnpo-SR* is a regulator of GSC establishment, GSC self-renewal, and the mitosis to meiosis transition during oogenesis. Loss of *Tnpo-SR* in GSCs results in decreased fusome area and decreased responsiveness to BMP signals, which likely both contribute to the ability of *Tnpo-SR*-depleted GSCs to self-renew. Loss of *Tnpo-SR* appears to suppress the mitotic-to-meiotic transition, resulting in egg chambers with variable numbers of germ cells, some of which remain mitotically active and undifferentiated, while others predominantly differentiate as nurse cells, but not oocytes. Finally, based on a targeted RNAi screen of related β-importins, we propose that the intracellular functions of *Tnpo-SR*, *cdm*, and *Ran* in germ cells are likely similar, as their loss of function results in similar germ cell counting defects and germ cell tumor formation.

Non-redundant functions of β-importins in the Drosophila germline may indicate their regulation of distinct sets of cargo proteins.

Although several α-importins have been implicated in oogenesis prior to our study (Geles and Adam, 2001; Mason et al., 2002; Máthé et al., 2000), this study is the first to identify a specific role for β-importins in germ cell mitotic expansion. Taken together with the recent discovery of *Importin 9* as a regulator of chromosome segregation, our data support the hypothesis that specific β-importins regulate distinct aspects of germ cell development (Hogarth et al., 2005; Mihalas et al., 2015; Nathaniel et al., 2021; Palacios et al., 2021). It is likely that we have not uncovered the breadth of β-importins necessary for germ cell function, nor the full extent of their functions. Indeed, our secondary screen for candidate β-importins is limited by our use of RNAi, which can be problematic, particularly in the

germline (DeLuca and Spradling, 2018; Ni et al., 2011). For example, Fs(2)Ket localizes at the nuclear envelope in dividing germ cells and *Fs(2)Ket* alleles are dominant female-sterile (Lippai et al., 2000; Tirián et al., 2000; Villanyi et al., 2008), yet we recovered embryos from *nosGal4::VP16>UAS-Fs(2)Ket^{RNAi}* mothers, indicating that maternal mRNA was not completely depleted. We also identified three germline-enhanced RNAi transgenes to knock-down expression of the β-importin encoded by *moleskin*, yet only one of the three yielded agametic ovaries, suggesting an off-target effect of the RNAi (Figure 7B, D). Future studies will need to employ other loss-of-function approaches to more thoroughly test the germline roles of other β-importins.

The repertoire of cargo carried by a β-importin determines its role in biological processes and its redundancy with other importins (Kimura and Imamoto, 2014). Although the full extent of protein-protein interactions mediated by *Drosophila* Tnpo-SR remains unknown, structural studies of the human ortholog TNPO3 identified binding partners involved in chromatin organization, mRNA and protein modification, cell cycle control, and cell-cell communication (Kimura et al., 2017; Maertens et al., 2014). Although β-importins were initially described for their ability to bind a consensus NLS, TNPO3 and Importin 13 (the human ortholog of Cadmus) can bind cargos lacking a NLS, instead relying on the unique three-dimensional interaction between the β-importin and its cargo (Kimura et al., 2021). One well-described set of Tnpo-SR cargoes are the SR-rich RNA binding proteins, which include essential regulators of mRNA splicing and transport (Allemand et al., 2002). Given that SR-rich proteins facilitate diverse RNA processing events, there are many potential Tnpo-SR cargo proteins that could influence cyst formation and GSC self-renewal, processes which are heavily influenced by translational control (Bradley et al., 2015; Carreira-Rosario et al., 2016; Teixeira and Lehmann, 2019). Our future studies will seek to identify Tnpo-SR and Cdm-interacting proteins, which should provide additional mechanistic details regarding how importins regulate germ cell mitotic expansion.

Tnpo-SR participates in the molecular regulation of germ cell differentiation.

The observation that depletion of *Tnpo-SR* results in variable numbers of germ cells per egg chamber and impaired oocyte differentiation suggests primary roles in germ cell differentiation. In *Drosophila*, as in many other organisms, germ cells develop as cysts of interconnected undifferentiated cells (Lu et al., 2017; Matova and Cooley, 2001; O'Connell and Pepling, 2021; Pepling and Lei, 2018). Cysts arise via incomplete cytokinesis, manifested by cleavage furrow arrest and the formation of stable ring canals that permit transport of cytoplasm and organelles (de Cuevas et al., 1997; Guertin et al., 2002; Haglund et al., 2011; Pepling and Lei, 2018). While knock-down of *Tnpo-SR* by RNAi led to >16 germ cells per egg chamber, we only rarely found examples of *Tnpo-SR^{GLC}* mutant egg chambers with more than 16 mutant germ cells; most had less than 16 cells, suggesting that progression through cyst divisions was impaired. We hypothesize that strong loss-of-function of *Tnpo-SR* in dividing cystoblasts causes these cells to undergo complete cytokinesis. In support of this model, we find that many mosaic germaria harboring cells with a strong loss of *Tnpo-SR* function contain a cluster of cells in the center of the germarium in which the fusome is aligned across individual cells, ring canal components are aligned between adjacent cells, and GFP-positive cytoplasm clearly extends between

cells. While it is possible that this phenotype represents a de-differentiation event, we have been unable to conclusively demonstrate that *Tnpo-SR* mutant germ cells mimic a cystoblast fate. Instead, we interpret this phenotype as a failure to maintain intracellular bridges between cyst cells. This is consistent with the results of weaker loss-of-function phenotypes, generated by expressing *Tnpo-SR* RNAi, where we observe some cyst formation, but also the formation of cystic germ cell tumors full of single or doublet germ cells. We speculate that in the *Tnpo-SR* RNAi model, delayed maturation of the fusomes creates weak connections between cells, resulting in premature abscission or collapsed intercellular bridges. Fragmented cysts are likely encapsulated along with adjacent cysts, thus yielding irregular (i.e., not 2^n) numbers of germ cells per cyst. That these cells manifest as single or doublet germ cells, rather than 4-cell cysts, may be the result of altered timing or different concentrations of the β-importins in the first division of the cystoblast versus the remaining three, perhaps reflecting differing sensitivity to abscission across the mitotic divisions (Mathieu et al., 2013; McKearin and Ohlstein, 1995). This may also be the reason why driving *Tnpo-SR* with *bam-Gal4* did not yield egg chambers with irregular numbers of germ cells, since UAS-reporter expression was not detectable in our hands until the 8-cell stage with this driver (Figure S1). However, we cannot completely rule out the possibility that the *bam-Gal4* drivers are not strong enough to fully deplete endogenous *Tnpo-SR* from 4- and 8-cell cysts. Future studies addressing the timing of Tnpo-SR action in mitotically dividing germ cells may yield important mechanistic insight into its function.

While additional studies will be necessary to tease apart the molecular mechanisms underlying the complex *Tnpo-SR* loss-of-function phenotypes, we hypothesize that one function of these particular β-importins in dividing germ cells is to suppress cytokinesis. Indeed, one function of β-importins in somatic cells is to partner with Ran to regulate mitotic spindle assembly, cell polarization, and contractile protein localization during cleavage furrow ingression (Beaudet et al., 2017; Ozugergin and Piekny, 2020; Sazer and Dasso, 2000; Silverman-Gavrila et al., 2008). Fusomes are composed of endoplasmic reticulum-like vesicles and cytoskeletal elements that originate from remnants of the mitotic spindle midbody (de Cuevas and Spradling, 1998; Koch and King, 1966; Koch et al., 1967; Lin and Spradling, 1995; Mahowald, 1971). Given that fusome area is greatly reduced in *Tnpo-SR*-depleted GSCs where the fusome is remodeled at every division, we speculate that Tnpo-SR promotes reorganization of the germ cell cytoskeleton after mitotic division, perhaps by shuttling cytoskeletal proteins back to the fusome or by controlling protein localization necessary to suppress cytokinesis in cyst cells. Our study raises important questions about the molecular connections between cell cycle control, cytokinesis, and the regulation of differentiation, which remain poorly characterized in germ cells.

Given the level of conservation in germ cell cyst formation across species, we propose that β-importins may also play important roles in higher eukaryotes, connecting the intricate programs of cell division, oocyte differentiation, and cell polarization. This may be of particular consequence for mouse and human oocytes, in which cyst breakdown occurs prior to meiotic onset (Pepling and Lei, 2018). Understanding how β-importins control cyst formation and breakdown may help elucidate how the oocyte reserve is established in humans, offering new potential avenues for treatment of infertility.

MATERIALS AND METHODS

Drosophila strains and husbandry

Flies were maintained at 22°–25°C in standard medium (cornmeal/molasses/yeast/agar) (NutriFly MF; Genesee Scientific). Female progeny were collected within 24 hours of eclosion and maintained on standard medium for 3, 6, and 10 days at 25°C; flies were fed wet yeast paste for 2–3 days (changed daily) prior to ovary dissection. *scrib^CA07683* (referred to as *Scrib::GFP*, a gift of A. Spradling) (Buszczak et al., 2007) and *Bam-sfGFP* (Vienna Drosophila Resource Center #v318001) (Sarov et al., 2016) were used to visualize fusomes and cytoplasmic Bam, respectively, in dividing cysts. *Dad-lacZ* (gifts from D. Drummond-Barbosa and T. Xie) was used to visualize activation of BMP signaling (Kai and Spradling, 2003; Song et al., 2004).

Construction of tagged Tnpo-SR alleles

Tnpo-SR::mCherry was engineered using CRISPR/Cas9 targeting of the *Tnpo-SR* locus by replacing the stop codon of *Tnpo-SR* with a *mCherry-3xP3-GFP* cassette containing an XbaI site, mCherry, and the floxed selection marker *3xP3-GFP*. The XbaI site adds a Ser Arg linker between *Tnpo-SR* and *mCherry*. Following Cre/loxP excision, a linker sequence of 46 bp remains between mCherry and the 3'UTR. Construction, screening, and Cre-mediated excision were performed by WellGenetics.

UAS-HA-Tnpo-SR was generated in *pUASz* for maximum expression in germline and soma (DeLuca and Spradling, 2018). Full-length *Tnpo-SR* cDNA was synthesized with three tandem HA tags in frame at the N-terminus and cloned into *pUC57mini* (GenScript). *HA-Tnpo-SR-pUC57mini* was linearized with SpeI and the *HA-Tnpo-SR* coding sequence cloned via InFusion cloning into *pUASz-1.0* (*Drosophila* Genetic Resource Center). Sanger sequencing was used to verify the coding sequence. Transgenic flies (*UASz-HA-Tnpo-SR*) were generated by phiC31 site-specific integrase into the *attP40* site on the second chromosome and the *attP2* site on the third chromosome (Bestgene).

Tissue-specific RNA interference (RNAi) generation

All RNAi lines used in this study were carried in *pVALIUM20* or *pVALIUM22* transgenes for maximum germline efficiency. *UAS-Tnpo-SR^RNAi* was generated as described (www.flyrnai.org/TRiP-HOME.html) (Ni et al., 2011). Primers were designed against the full-length *Tnpo-SR* RNA via the Designer of Small Interfering RNA tool (http://biodev.extra.cea.fr/DSIR/DSIRhtml) using default settings (21 nt siRNA; score threshold 90). A sequence with a score of 94.6 and 0 predicted off-targets was selected for hairpin generation (passenger strand, CGATCCCGTTTACTGGATAGA; guide strand, TCTATCCAGTAAACGGGATC). Primers were designed according to TRiP recommendations, annealed to form double-stranded oligos, and ligated into EcoRI-HF/NheI-HF-digested *pVALIUM22*. Transgenic flies (*UAS-Tnpo-SR^RNAi*) were generated by phiC31 site-specific integrase into the *attP2* site on the third chromosome (Bestgene).

For RNAi experiments, germline knock-down was facilitated by expressing the germline-specific *nos-GAL4::VP16-nos.UTR* (referred to throughout as *nos-Gal4*; BDSC #4937 or

7253) (Rørth, 1998; Van Doren et al., 1998) or *bam-Gal4::VP16* (referred to throughout as *bam-Gal4*; BDSC #80579) (Matias et al., 2015). Crosses and progeny were incubated at 25°C. Driver expression was confirmed using *UASp-tubGFP* (BDSC #7373) (Grieder et al., 2000). Females carrying drivers alone were used as controls. The following RNAi lines were also used for this study: *UAS-Pen^{GL01483}* (BDSC #43142), *UAS-Impβ11^{HMJ22418}* (RNAi-1; BDSC #58311), *UAS-Impβ11^{HMC03738}* (RNAi-2; BDSC #55142), *UAS-Tnpo^{HMS02968}* (BDSC #50732), *UAS-Tnpo/CG8219^{HMJ23009}* (BDSC #61230), *UAS-msk^{GL00435}* (RNAi-1; BDSC #35598), *UAS-msk^{HMS01408}* (RNAi-2; BDSC #34998), *UAS-msk^{HMS00020}* (RNAi-3; BDSC #33626), *UAS-emb^{HMS00991}* (BDSC #34021), *UAS-Fs(2)Ket^{GL01273}* (BDSC #41845), *UAS-cdm^{HMS02846}* (BDSC #44551), and *UAS-Ran^{GL01341}* (BDSC #42482).

Genetic mosaic generation

For genetic mosaic analyses using *flippase (FLP)/FLP recognition target (FRT)*, we obtained the following mutant alleles of *FRT*-containing chromosome arms: *Tnpo-SR^{KG04870}* [Kyoto *Drosophila* Stock Center (KDSC) #111581] (Bellen et al., 2004), *Tnpo-SR^{LL05552}* (KDSC #141628) (Schuldiner et al., 2008). Other genetic tools are described in FlyBase version FB2020_05 (Thurmond et al., 2019). Genetic mosaics were generated by *FLP/FRT*-mediated recombination in 2–3-day old females carrying a mutant allele in trans to a wildtype allele (linked to a *Ubi-GFP* marker) on homologous *FRT* arms, and a *hs-FLP* transgene, as described (Laws and Drummond-Barbosa, 2015). Flies were heat shocked at 37°C two times per day for 3 days and incubated at 25°C for 4, 8, or 12 days and supplemented with wet yeast paste on the last 2 days prior to dissection. Wild-type alleles were used for the generation of control (mock) mosaics.

Germ cell analyses

GSCs were identified based on the juxtaposition of their fusomes to the junction with adjacent cap cells (de Cuevas and Spradling, 1998). In *FLP/FRT* mutants, GSC loss was measured two ways. First, as the percentage of total mosaic germaria showing evidence of recent stem cell loss; namely, the presence of GFP-negative daughters (cystoblasts/cysts generated from an original GFP-negative stem cell) in the absence of the GFP-negative mother stem cell (Laws and Drummond-Barbosa, 2015). Second, as the percentage of total germaria analyzed that had at least one GFP-negative GSC. All results were subjected to Chi-Square analyses using Microsoft Excel. In RNAi progeny, GSC loss was measured as the average number of GSCs present over three timepoints. Results were subjected to Student's two-tailed T-test comparing driver controls versus *driver>UAS-RNAi* experimental groups at each timepoint individually using Microsoft Excel.

For analyses involving the egg chambers outside of the germarium, data was collected from the first three egg chambers posteriorly located from the germarium. Oocytes were identified by the presence of anti-Orb antibodies. The number of cells and ring canals per egg chamber were calculated based on visualization of ring canals with anti-pTyr and/or anti-Hts-RC antibodies and cell nuclei with DAPI. Results were subjected to Student's two-tailed T-test comparing driver controls versus *driver>UAS-RNAi* experimental groups at each timepoint individually using Microsoft Excel and Prism (GraphPad).

Immunofluorescence and microscopy

Ovaries were prepared for immunofluorescence microscopy as described (Grieder et al., 2000; Hinnant et al., 2017). In the standard protocol, ovaries were dissected and teased apart in Grace's medium without additives (Caisson Labs) and fixed in 5.3% formaldehyde in Grace's medium for 13 minutes at room temperature. They were then washed extensively in phosphate-buffered saline (PBS, pH 7.4; Fisher) with 0.1% Triton X-100, and blocked for three hours in blocking solution [5% bovine serum albumin (Sigma), 5% normal goat serum (MP Biomedicals), and 0.1% Triton X-100 in PBS] at room temperature. The following primary antibodies were diluted in blocking solution and used overnight at 4°C: chicken anti-GFP (#13970, Abcam; 1:2000), rabbit anti-phosphoHistone H3 (pHH3; #06–570, Millipore; 1:200), rat anti-E-Cadherin (DCAD2, Developmental Studies Hybridoma Bank (DSHB); 1:20), mouse anti-Orb (4H8 and 6H4; DSHB; 1:500), mouse anti-pTyrosine (pTyr; Millipore; 1:100), mouse anti-Hts-RC (DSHB; 1:10), and rabbit anti-C(3)G (a gift from M. Lilly; 1:3000). Primary antibodies mouse anti-Hts (1B1, DSHB; 1:10), and mouse anti-Lamin C (LC28.26, DSHB; 1:100) were incubated over two nights at 4°C. All primary antibodies are followed by a two hour incubation at room temperature with AlexaFluor 488-, 568- or 633-conjugated goat species-specific secondary antibodies (Life Technologies; 1:200).

All ovary samples were stained with 0.5 μg/ml 4'-6-diamidino-2-phenylindole (DAPI; Sigma) in 0.1% Triton X-100 in PBS, and mounted in 90% glycerol mixed with 20% n-propyl gallate (Sigma). Confocal z-stacks (1 μm optical sections) were collected with the Zeiss LSM700 laser scanning microscope using ZEN Black software. For imaging of Tnpo-SR::mCherry, low levels of protein required imaging 0.5 μm optical sections on a Zeiss LSM800 equipped with an AiryScan detector and post-processed using ZEN Blue software. Images were analyzed using Zeiss ZEN software, and minimally and equally enhanced via histogram using ZEN and Adobe Photoshop Creative Suite.

To compare Dad-lacZ levels between GSCs, fluorescence intensity was quantified using ZenBlue by manually demarcating individual GSC nuclei and measuring densitometric mean (grey units/pixel) at the largest nuclear diameter. E-cadherin levels at the GSC-cap cell junction in germline mosaics were similarly measured using morphometric analysis of single z-planes. Fusome area was measured in GSCs in single z-planes across their largest diameter. For all fluorescence intensity measurements, intensity was background-subtracted and normalized to an independent area of staining; statistical analysis was performed using the Student's two-tailed t-test with a Mann-Whitney post-test using GraphPad Prism.

Supplementary Material

Refer to Web version on PubMed Central for supplementary material.

ACKNOWLEDGMENTS

DATA AVAILABILITY

Fly strains and plasmids are available upon request. The authors affirm that all data necessary for confirming the conclusions of the article are present within the article and figures.

REFERENCES

Ables ET, Drummond-Barbosa D, 2013. Cyclin E controls Drosophila female germline stem cell maintenance independently of its role in proliferation by modulating responsiveness to niche signals. Development 140, 530–540. [PubMed: 23293285]

Ables ET, Hwang GH, Finger DS, Hinnant TD, Drummond-Barbosa D, 2016. A Genetic Mosaic Screen Reveals Ecdysone-Responsive Genes Regulating Drosophila Oogenesis. G3 (Bethesda, Md.) 6, 2629–2642. [PubMed: 27226164]

Allemand E, Dokudovskaya S, Bordonné R, Tazi J, 2002. A conserved Drosophila transportin-serine/arginine-rich (SR) protein permits nuclear import of Drosophila SR protein splicing factors and their antagonist repressor splicing factor 1. Molecular biology of the cell 13, 2436–2447. [PubMed: 12134081]

Beaudet D, Akhshi T, Phillipp J, Law C, Piekny A, 2017. Active Ran regulates anillin function during cytokinesis. Molecular biology of the cell 28, 3517–3531. [PubMed: 28931593]

Bellen HJ, Levis RW, Liao G, He Y, Carlson JW, Tsang G, Evans-Holm M, Hiesinger PR, Schulze KL, Rubin GM, Hoskins RA, Spradling AC, 2004. The BDGP gene disruption project: single transposon insertions associated with 40% of Drosophila genes. Genetics 167, 761–781. [PubMed: 15238527]

Bradley T, Cook ME, Blanchette M, 2015. SR proteins control a complex network of RNA-processing events. Rna 21, 75–92. [PubMed: 25414008]

Buszczak M, Paterno S, Lighthouse D, Bachman J, Planck J, Owen S, Skora AD, Nystul TG, Ohlstein B, Allen A, Wilhelm JE, Murphy TD, Levis RW, Matunis E, Srivali N, Hoskins RA, Spradling AC, 2007. The carnegie protein trap library: a versatile tool for Drosophila developmental studies. Genetics 175, 1505–1531. [PubMed: 17194782]

Carreira-Rosario A, Bhargava V, Hillebrand J, Kollipara RK, Ramaswami M, Buszczak M, 2016. Repression of Pumilio Protein Expression by Rbfox1 Promotes Germ Cell Differentiation. Developmental cell 36, 562–571. [PubMed: 26954550]

Cautain B, Hill R, de Pedro N, Link W, 2015. Components and regulation of nuclear transport processes. The FEBS journal 282, 445–462. [PubMed: 25429850]

Chen D, McKearin D, 2003. Dpp signaling silences bam transcription directly to establish asymmetric divisions of germline stem cells. Current biology : CB 13, 1786–1791. [PubMed: 14561403]

Chen D, Wang Q, Huang H, Xia L, Jiang X, Kan L, Sun Q, Chen D, 2009. Effete-mediated degradation of Cyclin A is essential for the maintenance of germline stem cells in Drosophila. Development 136, 4133–4142. [PubMed: 19906849]

Clémot M, Molla-Herman A, Mathieu J, Huynh JR, Dostatni N, 2018. The replicative histone chaperone CAF1 is essential for the maintenance of identity and genome integrity in adult stem cells. Development 145.

de Cuevas M, Lilly MA, Spradling AC, 1997. Germline cyst formation in Drosophila. Annual review of genetics 31, 405–428.

de Cuevas M, Spradling AC, 1998. Morphogenesis of the Drosophila fusome and its implications for oocyte specification. Development 125, 2781–2789. [PubMed: 9655801]

DeLuca SZ, Spradling AC, 2018. Efficient Expression of Genes in the Drosophila Germline Using a UAS Promoter Free of Interference by Hsp70 piRNAs. Genetics 209, 381–387. [PubMed: 29669732]

Deng W, Lin H, 1997. Spectrosomes and fusomes anchor mitotic spindles during asymmetric germ cell divisions and facilitate the formation of a polarized microtubule array for oocyte specification in Drosophila. Developmental biology 189, 79–94. [PubMed: 9281339]

Eikenes Å H, Malerød L, Lie-Jensen A, Sem Wegner C, Brech A, Liestøl K, Stenmark H, Haglund K, 2015. Src64 controls a novel actin network required for proper ring canal formation in the Drosophila male germline. Development 142, 4107–4118. [PubMed: 26628094]

Geles KG, Adam SA, 2001. Germline and developmental roles of the nuclear transport factor importin alpha3 in C. elegans. Development 128, 1817–1830. [PubMed: 11311162]

Grieder NC, de Cuevas M, Spradling AC, 2000. The fusome organizes the microtubule network during oocyte differentiation in Drosophila. Development 127, 4253–4264. [PubMed: 10976056]

Guertin DA, Trautmann S, McCollum D, 2002. Cytokinesis in eukaryotes. Microbiology and molecular biology reviews : MMBR 66, 155–178. [PubMed: 12040122]

Haglund K, Nezis IP, Stenmark H, 2011. Structure and functions of stable intercellular bridges formed by incomplete cytokinesis during development. Communicative & integrative biology 4, 1–9. [PubMed: 21509167]

Hinnant TD, Alvarez AA, Ables ET, 2017. Temporal remodeling of the cell cycle accompanies differentiation in the Drosophila germline. Developmental biology 429, 118–131. [PubMed: 28711427]

Hinnant TD, Merkle JA, Ables ET, 2020. Coordinating Proliferation, Polarity, and Cell Fate in the Drosophila Female Germline. Frontiers in cell and developmental biology 8, 19.

Hogarth C, Itman C, Jans DA, Loveland KL, 2005. Regulated nucleocytoplasmic transport in spermatogenesis: a driver of cellular differentiation? BioEssays : news and reviews in molecular, cellular and developmental biology 27, 1011–1025. [PubMed: 16163727]

Hughes SE, Miller DE, Miller AL, Hawley RS, 2018. Female Meiosis: Synapsis, Recombination, and Segregation in Drosophila melanogaster. Genetics 208, 875–908. [PubMed: 29487146]

Huynh J-R, 2006. Fusome as a Cell-Cell Communication Channel of Drosophila Ovarian Cyst, in: Baluska F, Volkmann D, Barlow PW (Eds.), Cell-Cell Channels. Springer New York, New York, NY, pp. 217–235.

Ji S, Li C, Hu L, Liu K, Mei J, Luo Y, Tao Y, Xia Z, Sun Q, Chen D, 2017. Bam-dependent deubiquitinase complex can disrupt germ-line stem cell maintenance by targeting cyclin A. Proceedings of the National Academy of Sciences of the United States of America 114, 6316–6321. [PubMed: 28484036]

Kai T, Spradling A, 2003. An empty Drosophila stem cell niche reactivates the proliferation of ectopic cells. Proc Natl Acad Sci U S A 100, 4633–4638. [PubMed: 12676994]

Kataoka N, Bachorik JL, Dreyfuss G, 1999. Transportin-SR, a nuclear import receptor for SR proteins. J Cell Biol 145, 1145–1152. [PubMed: 10366588]

Kimura M, Imai K, Morinaka Y, Hosono-Sakuma Y, Horton P, Imamoto N, 2021. Distinct mutations in importin-β family nucleocytoplasmic transport receptors transportin-SR and importin-13 affect specific cargo binding. Sci Rep 11, 15649. [PubMed: 34341383]

Kimura M, Imamoto N, 2014. Biological significance of the importin-β family-dependent nucleocytoplasmic transport pathways. Traffic (Copenhagen, Denmark) 15, 727–748. [PubMed: 24766099]

Kimura M, Morinaka Y, Imai K, Kose S, Horton P, Imamoto N, 2017. Extensive cargo identification reveals distinct biological roles of the 12 importin pathways. eLife 6.

King RCRC, 1970. Ovarian development in Drosophila melanogaster. Academic Press, New York.

Koch EA, King RC, 1966. The origin and early differentiation of the egg chamber of Drosophila melanogaster. J Morphol 119, 283–303. [PubMed: 5967290]

Koch EA, Smith PA, King RC, 1967. The division and differentiation of Drosophila cystocytes. J Morphol 121, 55–70. [PubMed: 6031719]

Lai MC, Lin RI, Tarn WY, 2001. Transportin-SR2 mediates nuclear import of phosphorylated SR proteins. Proc Natl Acad Sci U S A 98, 10154–10159. [PubMed: 11517331]

Laws KM, Drummond-Barbosa D, 2015. Genetic Mosaic Analysis of Stem Cell Lineages in the Drosophila Ovary. Methods in molecular biology (Clifton, N.J.) 1328, 57–72.

Lehmann R, 2012. Germline Stem Cells: Origin and Destiny. Cell stem cell 10, 729–739. [PubMed: 22704513]

Lighthouse DV, Buszczak M, Spradling AC, 2008. New components of the Drosophila fusome suggest it plays novel roles in signaling and transport. Developmental biology 317, 59–71. [PubMed: 18355804]

Lilly MA, de Cuevas M, Spradling AC, 2000. Cyclin A associates with the fusome during germline cyst formation in the Drosophila ovary. Developmental biology 218, 53–63. [PubMed: 10644410]

Lin H, Spradling AC, 1995. Fusome asymmetry and oocyte determination in Drosophila. Dev Genet 16, 6–12. [PubMed: 7758245]

Lin H, Yue L, Spradling AC, 1994. The Drosophila fusome, a germline-specific organelle, contains membrane skeletal proteins and functions in cyst formation. Development 120, 947–956. [PubMed: 7600970]

Lippai M, Tirián L, Boros I, Mihály J, Erdélyi M, Belecz I, Máthé E, Pósfai J, Nagy A, Udvardy A, Paraskeva E, Görlich D, Szabad J, 2000. The Ketel gene encodes a Drosophila homologue of importin-beta. Genetics 156, 1889–1900. [PubMed: 11102382]

Liu T, Wang Q, Li W, Mao F, Yue S, Liu S, Liu X, Xiao S, Xia L, 2017. Gcn5 determines the fate of Drosophila germline stem cells through degradation of Cyclin A. Faseb j 31, 2185–2194. [PubMed: 28188175]

Lu K, Jensen L, Lei L, Yamashita YM, 2017. Stay Connected: A Germ Cell Strategy. Trends in genetics : TIG 33, 971–978. [PubMed: 28947158]

Maertens GN, Cook NJ, Wang W, Hare S, Gupta SS, Öztop I, Lee K, Pye VE, Cosnefroy O, Snijders AP, KewalRamani VN, Fassati A, Engelman A, Cherepanov P, 2014. Structural basis for nuclear import of splicing factors by human Transportin 3. Proc Natl Acad Sci U S A 111, 2728–2733. [PubMed: 24449914]

Mahowald AP, 1971. The formation of ring canals by cell furrows in Drosophila. Z Zellforsch Mikrosk Anat 118, 162–167. [PubMed: 4937106]

Mason DA, Fleming RJ, Goldfarb DS, 2002. Drosophila melanogaster importin alpha1 and alpha3 can replace importin alpha2 during spermatogenesis but not oogenesis. Genetics 161, 157–170. [PubMed: 12019231]

Mason DA, Goldfarb DS, 2009. The nuclear transport machinery as a regulator of Drosophila development. Seminars in cell & developmental biology 20, 582–589. [PubMed: 19508860]

Máthé E, Bates H, Huikeshoven H, Deák P, Glover DM, Cotterill S, 2000. Importin-alpha3 is required at multiple stages of Drosophila development and has a role in the completion of oogenesis. Developmental biology 223, 307–322. [PubMed: 10882518]

Mathieu J, Cauvin C, Moch C, Radford SJ, Sampaio P, Perdigoto CN, Schweisguth F, Bardin AJ, Sunkel CE, McKim K, Echard A, Huynh JR, 2013. Aurora B and cyclin B have opposite effects on the timing of cytokinesis abscission in Drosophila germ cells and in vertebrate somatic cells. Developmental cell 26, 250–265. [PubMed: 23948252]

Matias NR, Mathieu J, Huynh JR, 2015. Abscission is regulated by the ESCRT-III protein shrub in Drosophila germline stem cells. PLoS genetics 11, e1004653. [PubMed: 25647097]

Matova N, Cooley L, 2001. Comparative aspects of animal oogenesis. Developmental biology 231, 291–320. [PubMed: 11237461]

McKearin D, 1997. The Drosophila fusome, organelle biogenesis and germ cell differentiation: if you build it. BioEssays : news and reviews in molecular, cellular and developmental biology 19, 147–152. [PubMed: 9046244]

McKearin D, Ohlstein B, 1995. A role for the Drosophila bag-of-marbles protein in the differentiation of cystoblasts from germline stem cells. Development 121, 2937–2947. [PubMed: 7555720]

Mihalas BP, Western PS, Loveland KL, McLaughlin EA, Holt JE, 2015. Changing expression and subcellular distribution of karyopherins during murine oogenesis. Reproduction (Cambridge, England) 150, 485–496. [PubMed: 26399853]

Morris JZ, Hong A, Lilly MA, Lehmann R, 2005. twin, a CCR4 homolog, regulates cyclin poly(A) tail length to permit Drosophila oogenesis. Development 132, 1165–1174. [PubMed: 15703281]

Nachury MV, Maresca TJ, Salmon WC, Waterman-Storer CM, Heald R, Weis K, 2001. Importin beta is a mitotic target of the small GTPase Ran in spindle assembly. Cell 104, 95–106. [PubMed: 11163243]

Nathaniel B, Whiley PAF, Miyamoto Y, Loveland KL, 2021. Importins: Diverse roles in male fertility. Seminars in cell & developmental biology.

Nguyen LTS, Robinson DN, 2020. The Unusual Suspects in Cytokinesis: Fitting the Pieces Together. Frontiers in cell and developmental biology 8, 441. [PubMed: 32626704]

Ni JQ, Zhou R, Czech B, Liu LP, Holderbaum L, Yang-Zhou D, Shim HS, Tao R, Handler D, Karpowicz P, Binari R, Booker M, Brennecke J, Perkins LA, Hannon GJ, Perrimon N, 2011. A genome-scale shRNA resource for transgenic RNAi in Drosophila. Nat Methods 8, 405–407. [PubMed: 21460824]

O'Connell JM, Pepling ME, 2021. Primordial Follicle Formation - Some Assembly Required. Curr Opin Endocr Metab Res 18, 118–127. [PubMed: 34027225]

Ohlmeyer JT, Schüpbach T, 2003. Encore facilitates SCF-Ubiquitin-proteasome-dependent proteolysis during Drosophila oogenesis. Development 130, 6339–6349. [PubMed: 14623823]

Okada N, Ishigami Y, Suzuki T, Kaneko A, Yasui K, Fukutomi R, Isemura M, 2008. Importins and exportins in cellular differentiation. J Cell Mol Med 12, 1863–1871. [PubMed: 18657223]

Ong S, Tan C, 2010. Germline cyst formation and incomplete cytokinesis during Drosophila melanogaster oogenesis. Developmental biology 337, 84–98. [PubMed: 19850028]

Ozugergin I, Piekny A, 2020. Complementary functions for the Ran gradient during division. Small GTPases, 1–11. [PubMed: 29363391]

Palacios V, Kimble GC, Tootle TL, Buszczak M, 2021. Importin-9 regulates chromosome segregation and packaging in Drosophila germ cells. J Cell Sci 134.

Pan L, Chen S, Weng C, Call G, Zhu D, Tang H, Zhang N, Xie T, 2007. Stem cell aging is controlled both intrinsically and extrinsically in the Drosophila ovary. Cell Stem Cell 1, 458–469. [PubMed: 18371381]

Pepling M, Lei L, 2018. Germ Cell Nests and Germline Cysts, in: Skinner MK (Ed.), Encyclopedia of Reproduction (Second Edition). Academic Press, Oxford, pp. 159–166.

Quan Y, Ji ZL, Wang X, Tartakoff AM, Tao T, 2008. Evolutionary and transcriptional analysis of karyopherin beta superfamily proteins. Molecular & cellular proteomics : MCP 7, 1254–1269. [PubMed: 18353765]

Röper K, 2007. Rtnl1 is enriched in a specialized germline ER that associates with ribonucleoprotein granule components. J Cell Sci 120, 1081–1092. [PubMed: 17327273]

Rørth P, 1998. Gal4 in the Drosophila female germline. Mech Dev 78, 113–118. [PubMed: 9858703]

Sarov M, Barz C, Jambor H, Hein MY, Schmied C, Suchold D, Stender B, Janosch S, V. K,J, Krishnan RT, Krishnamoorthy A, Ferreira IR, Ejsmont RK, Finkl K, Hasse S, Kämpfer P, Plewka N, Vinis E, Schloissnig S, Knust E, Hartenstein V, Mann M, Ramaswami M, VijayRaghavan K, Tomancak P, Schnorrer F, 2016. A genome-wide resource for the analysis of protein localisation in Drosophila. eLife 5, e12068. [PubMed: 26896675]

Sazer S, Dasso M, 2000. The ran decathlon: multiple roles of Ran. J Cell Sci 113 (Pt 7), 1111–1118. [PubMed: 10704362]

Schuldiner O, Berdnik D, Levy JM, Wu JS, Luginbuhl D, Gontang AC, Luo L, 2008. piggyBac-based mosaic screen identifies a postmitotic function for cohesin in regulating developmental axon pruning. Developmental cell 14, 227–238. [PubMed: 18267091]

Silverman-Gavrila RV, Hales KG, Wilde A, 2008. Anillin-mediated targeting of peanut to pseudocleavage furrows is regulated by the GTPase Ran. Molecular biology of the cell 19, 3735–3744. [PubMed: 18579688]

Slaidina M, Gupta S, Banisch TU, Lehmann R, 2021. A single-cell atlas reveals unanticipated cell type complexity in Drosophila ovaries. Genome Res 31, 1938–1951. [PubMed: 34389661]

Snapp EL, Iida T, Frescas D, Lippincott-Schwartz J, Lilly MA, 2004. The fusome mediates intercellular endoplasmic reticulum connectivity in Drosophila ovarian cysts. Molecular biology of the cell 15, 4512–4521. [PubMed: 15292454]

Song X, Wong MD, Kawase E, Xi R, Ding BC, McCarthy JJ, Xie T, 2004. Bmp signals from niche cells directly repress transcription of a differentiation-promoting gene, bag of marbles, in germline stem cells in the Drosophila ovary. Development 131, 1353–1364. [PubMed: 14973291]

Song X, Zhu C-H, Doan C, Xie T, 2002. Germline Stem Cells Anchored by Adherens Junctions in the *Drosophila* Ovary Niches. Science 296, 1855–1857. [PubMed: 12052957]

Soniat M, Chook YM, 2015. Nuclear localization signals for four distinct karyopherin-β nuclear import systems. Biochem J 468, 353–362. [PubMed: 26173234]

Sugimura I, Lilly MA, 2006. Bruno inhibits the expression of mitotic cyclins during the prophase I meiotic arrest of Drosophila oocytes. Developmental cell 10, 127–135. [PubMed: 16399084]

Teixeira FK, Lehmann R, 2019. Translational Control during Developmental Transitions. Cold Spring Harb Perspect Biol 11.

Thurmond J, Goodman JL, Strelets VB, Attrill H, Gramates LS, Marygold SJ, Matthews BB, Millburn G, Antonazzo G, Trovisco V, Kaufman TC, Calvi BR, 2019. FlyBase 2.0: the next generation. Nucleic Acids Res 47, D759–d765. [PubMed: 30364959]

Tirián L, Puro J, Erdélyi M, Boros I, Papp B, Lippai M, Szabad J, 2000. The Ketel(D) dominant-negative mutations identify maternal function of the Drosophila importin-beta gene required for cleavage nuclei formation. Genetics 156, 1901–1912. [PubMed: 11102383]

Van Doren M, Williamson AL, Lehmann R, 1998. Regulation of zygotic gene expression in Drosophila primordial germ cells. Current biology : CB 8, 243–246. [PubMed: 9501989]

Villa-Fombuena G, Lobo-Pecellín M, Marín-Menguiano M, Rojas-Ríos P, González-Reyes A, 2021. Live imaging of the Drosophila ovarian niche shows spectrosome and centrosome dynamics during asymmetric germline stem cell division. Development 148.

Villanyi Z, Papp B, Szikora S, Boros I, Szabad J, 2008. The DRE motif is a key component in the expression regulation of the importin-beta encoding Ketel gene in Drosophila. Mech Dev 125, 822–831. [PubMed: 18656533]

Xie T, Spradling AC, 1998. decapentaplegic is essential for the maintenance and division of germline stem cells in the Drosophila ovary. Cell 94, 251–260. [PubMed: 9695953]

Xu T, Rubin GM, 1993. Analysis of genetic mosaics in developing and adult Drosophila tissues. Development 117, 1223–1237. [PubMed: 8404527]

Yamashita YM, 2018. Subcellular Specialization and Organelle Behavior in Germ Cells. Genetics 208, 19–51. [PubMed: 29301947]

SUMMARY STATEMENT

β-importin Tnpo-SR promotes germline stem cell maintenance and germ cell development in the *Drosophila* ovary.

HIGHLIGHTS

- β-importin *Tnpo-SR* is necessary for *Drosophila* female germ cell development

- Tnpo-SR localizes to nuclei in germline stem cells and mitotically-dividing cysts

- Loss of *Tnpo-SR* depletes germline stem cells

- Loss of *Tnpo-SR* suppresses the mitotic-meiotic transition
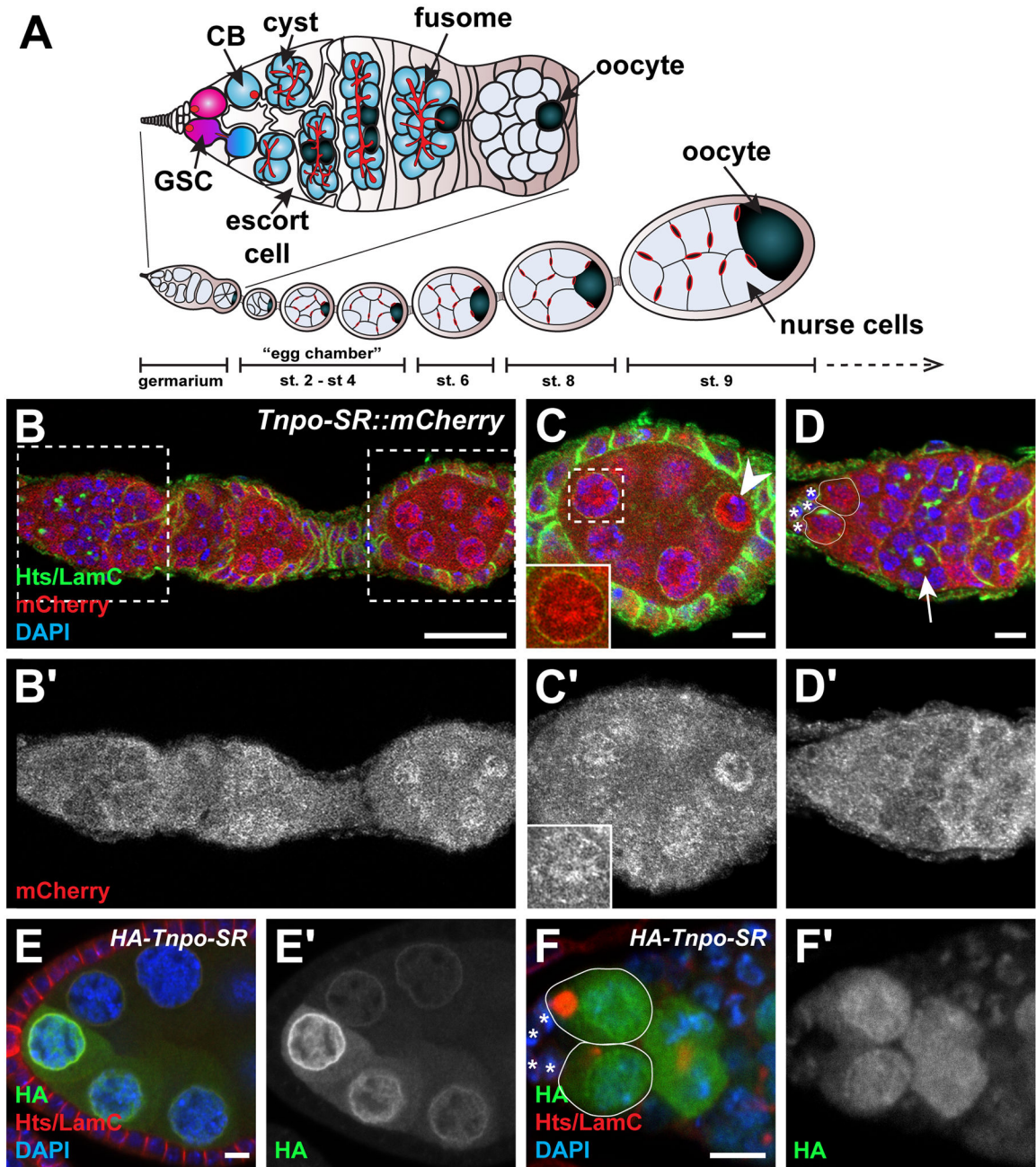
Figure 1. Tnpo-SR is expressed in the *Drosophila* ovary and localizes to the nucleus, nuclear membrane, and cytoplasm.

(A) The *Drosophila* ovary is composed of ovarioles harboring a germarium (top) and older egg chambers containing developing oocytes (bottom). In the germarium, germline stem cells (GSCs; pink) are adjacent to cap cells and escort cells. GSCs divide to form cystoblasts (CB; blue) that divide four times to form 16-cell cysts (blue). Cysts are composed of 15 nurse cells and one oocyte (dark blue), connected by 15 intercellular bridges that can be visualized by ring canals and the fusome (red) that transects each bridge. (B-D') *TnpoSR::mCherry* ovariole labeled with anti-mCherry (red), anti-Hts (green), anti-LamC (green) and DAPI (blue). Regions boxed in B are magnified in C (stage 3 egg

chamber) and D (anterior tip of the germarium). Region boxed in C is enlarged in the inset. Grayscale images of the corresponding red channel alone in B'-D'. Arrowhead in C indicates the oocyte; arrow in D points to an 8-cell cyst. (E-F') Stage 6 egg chamber (E) and anterior tip of the germarium (F) from a *nos-Gal4::VP16>HA-TnpoSR* ovariole labeled with anti-HA (green), anti-Hts (red), anti-LamC (red) and DAPI (blue). Grayscale images of the corresponding green channel alone in E'-F'. Lines demarcate GSCs (white); asterisks indicate cap cells. Scale bars = 20 μm (B) or 5 μm (C-F).
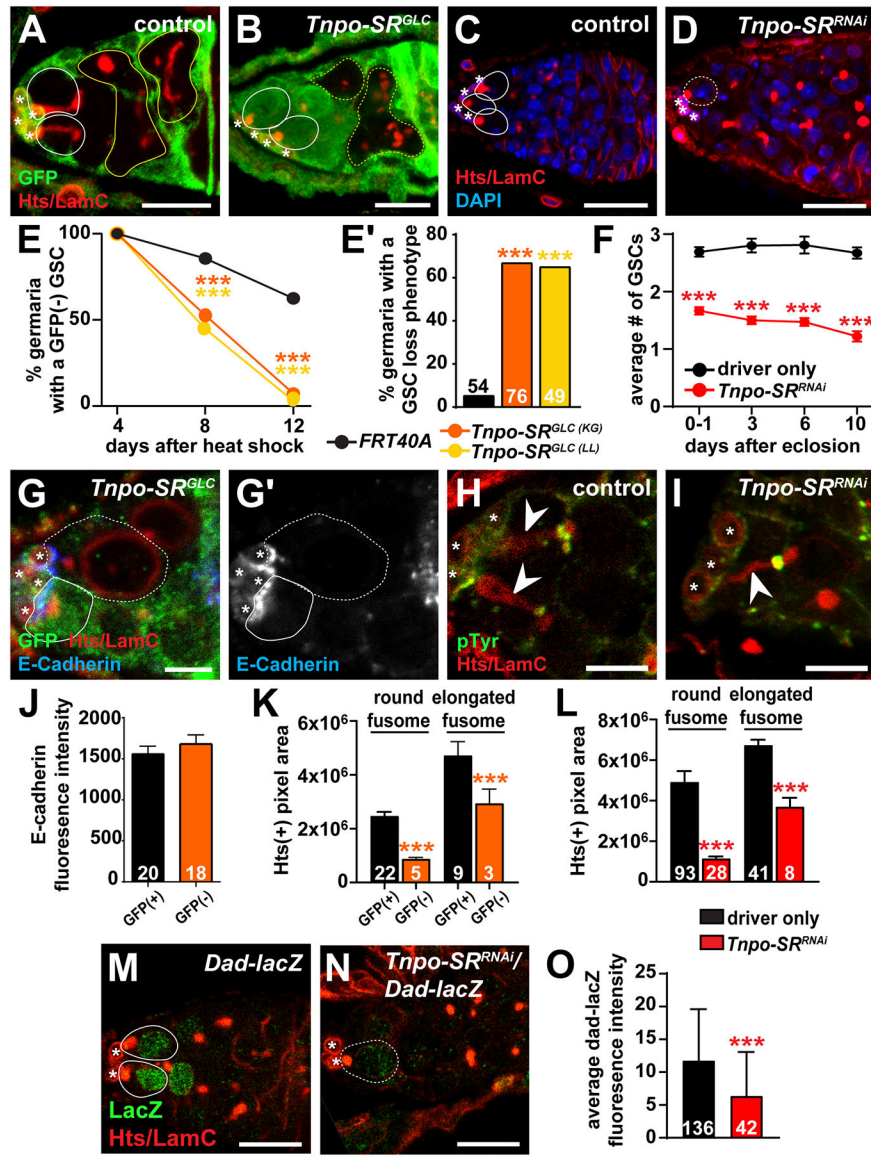
Figure 2. *Tnpo-SR* **is necessary for GSC establishment and maintenance.**

(A-B) Germline mosaic germaria from control (*FRT40A*; A) and *Tnpo-SR^{GLC}* mutant females 8 days after heat shock labeled with anti-GFP (green), anti-Hts (red), and anti-LamC (red). (C-D) *nos-Gal4* control (C) and *nos-Gal4>Tnpo-SR^{RNAi}* (D) germaria labeled with anti-Hts (red), anti-LamC (red), and DAPI (blue). (E-E') Germline stem cell loss was measured as the percentage of total germaria with a GFP-negative GSC at 4, 8, and 12 days after clone induction (E; n = at least 50 germaria per timepoint) or as the number of germline-mosaic germaria with a GSC loss phenotype (E'; numbers in the bars represent total number of germaria analyzed). (F) Average number of GSCs per germarium in *nos-Gal4* control or *nos-Gal4>Tnpo-SR^{RNAi}* ovaries. More than 50 germaria from at least 40 females were analyzed per timepoint. (G-G', J). *Tnpo-SR^{GLC}* mutant mosaic germaria at 8 days after clone induction labeled with anti-GFP (green; wild-type cells), anti-Hts (red), anti-LamC (red), and anti-E-cadherin (blue; image in G' is blue channel alone). Average

fluorescence intensity of E-cadherin at the GSC-cap cell junction is shown in J. (H-I, K-L) Comparison of fusome architecture in driver control (H) and *nos-Gal4>Tnpo-SR^{RNAi}* (I) germaria labeled with anti-pTyrosine (for ring canal proteins; green), anti-Hts (red), and anti-LamC (red). Hts-positive pixel area was used as a measure of fusome area in round or elongated fusomes in wild-type, *Tnpo-SR^{GLC}* mutant (K) or *Tnpo-SR^{RNAi}* (L) GSCs. (M-O) *Dad-lacZ* expression in driver control (M) and *nos-Gal4>Tnpo-SR^{RNAi}* (N) germaria labeled with anti-β-gal (for *dad-lacZ*, green), anti-Hts (red), and anti-LamC (red). Average fluorescence intensity for *dad-lacZ* is quantified in O. Lines demarcate wild-type (solid) or mutant (dashed) GSCs (white) and cystoblast/cysts (yellow); asterisks indicate cap cells. Scale bars = 10 μm. ***$p < 0.001$, Student's two-tailed t-test (E, F), t-test with Mann-Whitney post-test (J-L, O), or Chi-square test (E'). Numbers in the bars (J-L, O) represent the total number of GSCs analyzed. All images of *Tnpo-SR^{GLC}* GSCs are from *Tnpo-SR^{KG}* females. Error bars represent s.e.m.
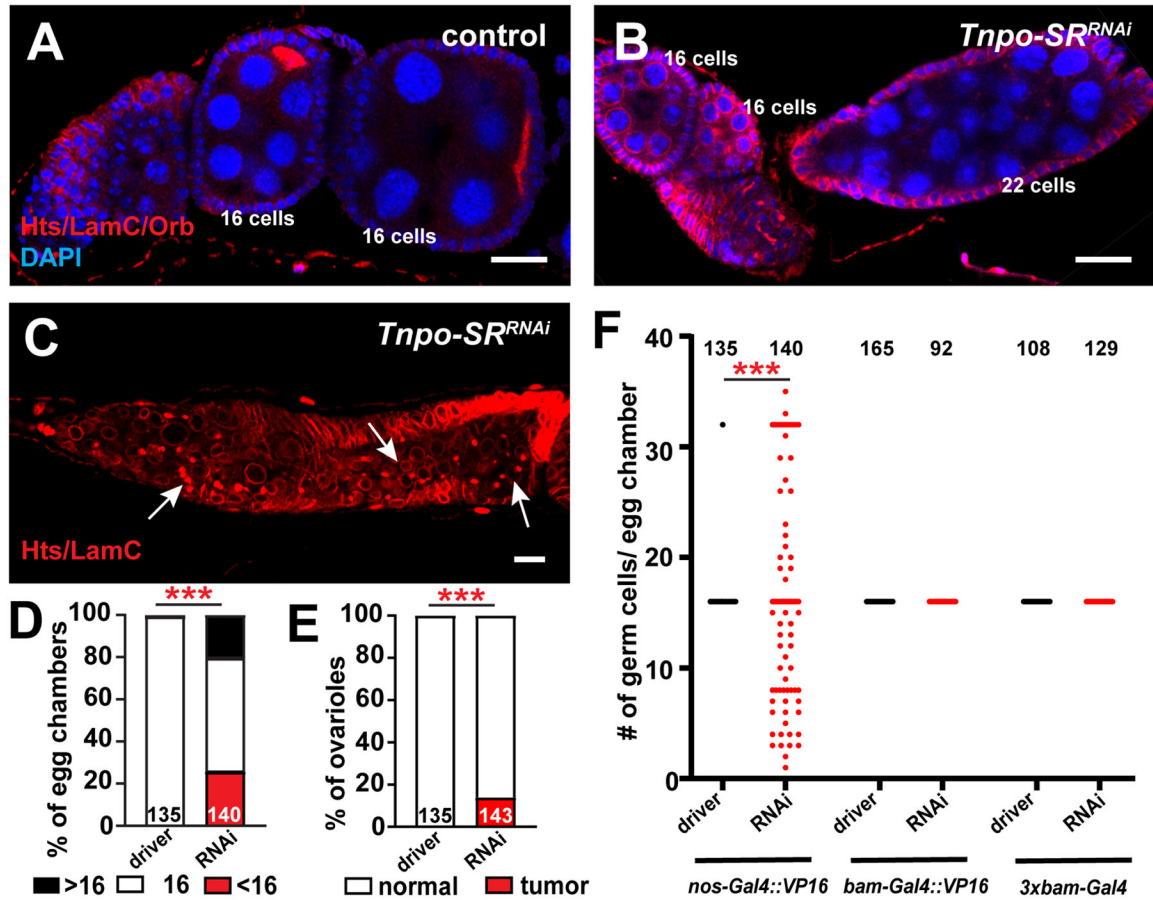
Figure 3. Loss of *Tnpo-SR* from germ cells alters the number of germ cells per egg chamber.
(A-C) *nos-Gal4* driver control (A) or *nos-Gal4>Tnpo-SR^{RNAi}* (B-C) germaria labeled with anti-Hts (red), anti-LamC (red), anti-Orb (red), and DAPI (blue, A-B). Scale bars, 20 μm. (D-E) Penetrance of egg chamber phenotypes was quantified as the frequencies of egg chambers containing less than 16 (red), 16 (white), or more than 16 (black) germ cells per egg chamber (D) or the frequency of tumorous egg chambers (red, E) in *nos-Gal4* control or *nos-Gal4>Tnpo-SR^{RNAi}* at six days after eclosion. (F) Ovarioles expressing *Tnpo-SR^{RNAi}* driven with *nos-Gal4*, *bam-Gal4*, or a triple *bam-Gal4* driver (*3xbam-Gal4)* were immunostained with anti-Hts, anti-LamC, and DAPI, and quantified for the number of germ cells per egg chamber. Each dot represents one egg chamber. Numbers in bars (D-E) or above dots (F) represent the total number of egg chambers analyzed. ***$p < 0.001$; Chi-square test (D-E) or Kolmogorov-Smirnov test to assess the spread of datapoints (F).
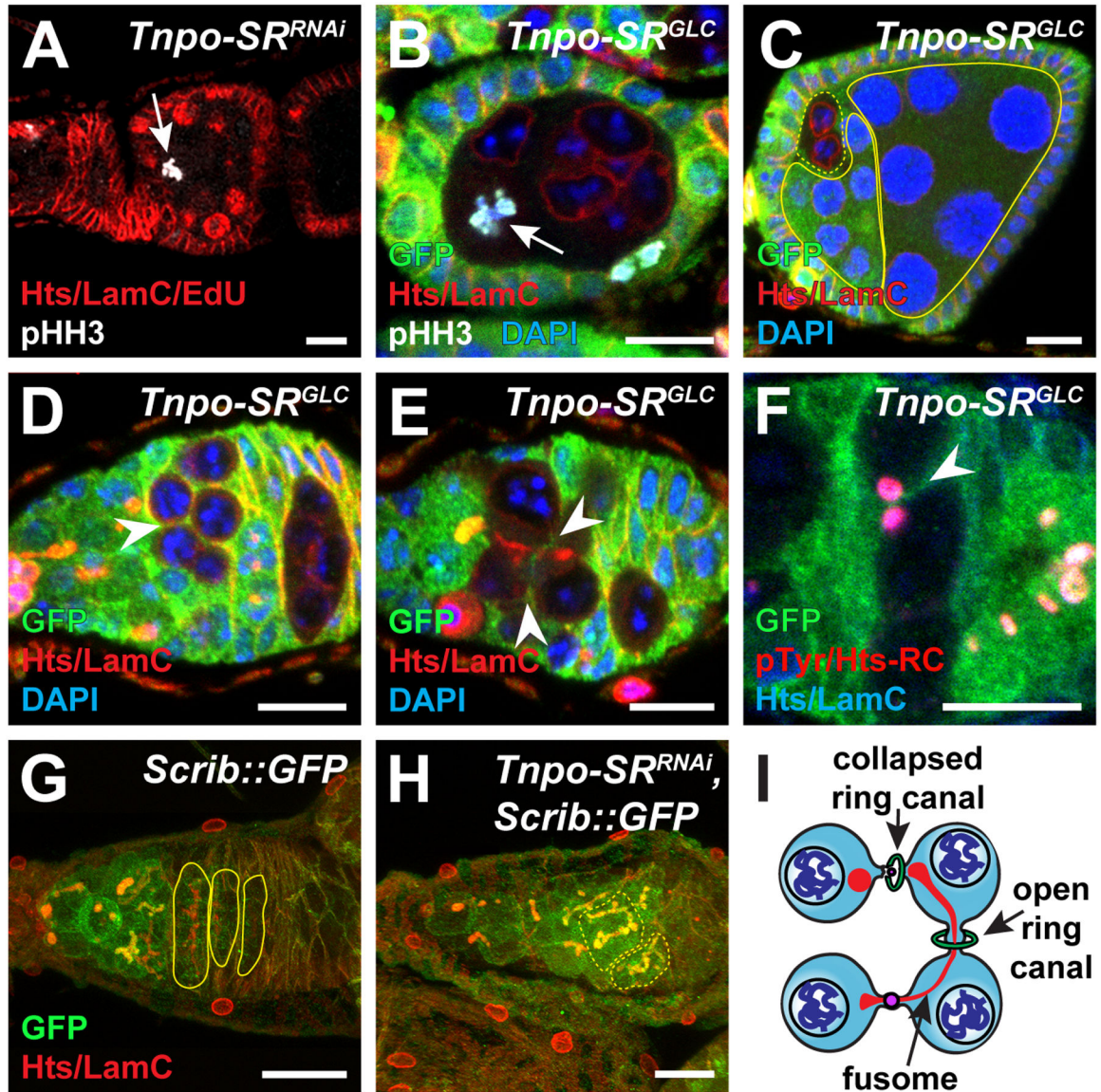
Figure 4. *Tnpo-SR*-depleted germ cells remain mitotically active and undifferentiated and appear to fragment into singlet and doublet clusters.

(A-B) *nos-Gal4>Tnpo-SR^{RNAi}* (A) and *Tnpo-SR^{GLC}* mutant mosaic (B) egg chambers labeled with anti-pHistone-H3 (pHH3; white), anti-Hts (red), anti-LamC (red), the S-phase marker EdU (A only; red), anti-GFP (B only; green; wild-type cells), and DAPI (blue). (C-E) *Tnpo-SR^{GLC}* mutant mosaic egg chamber (C) or germaria (D-E) labeled with anti-GFP (green; wild-type cells), anti-Hts (red), anti-LamC (red), and DAPI (blue). (F) *Tnpo-SR^{GLC}* mutant germarium labeled with anti-GFP (green; wild-type cells), anti-Hts-RC and anti-pTyr (to label ring canal proteins; red), and anti-Hts with anti-LamC (blue). Note the thin thread of GFP+ material between the two ring canals. Arrowheads indicate the GFP+ somatic cell projections invaginating the mutant cysts. (G-H) *Scrib::GFP* control (G) and *nos-Gal4>Tnpo-SR^{RNAi};Scrib::GFP* (H) germaria labeled with anti-GFP (for *Scrib::GFP*; green), anti-Hts (red), and anti-LamC (red). (I) Model depicting potential mechanism for cyst fragmentation in *Tnpo-SR*-depleted germ cells (blue, germ cells; red, fusome). Images

in panels B-C and F were collected from *Tnpo-SR*^{KG} females, and images in panels D-E were collected from *Tnpo-SR*^{LL} females.
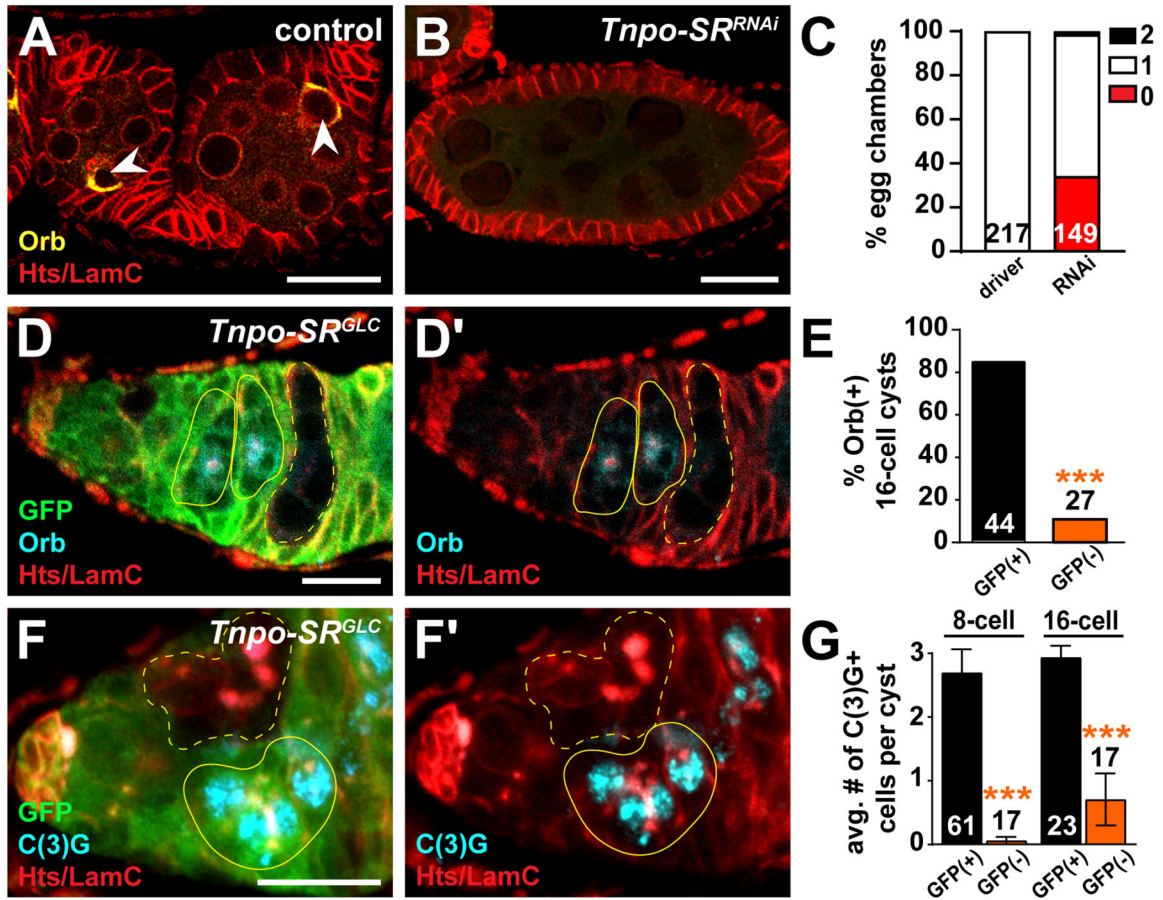
Figure 5. *Tnpo-SR*-depleted germ cells do not properly accumulate oocyte-specific proteins.
(A-C) Driver control (A) and *nos-Gal4>Tnpo-SR^{RNAi}* (B) egg chambers labeled with anti-Orb (yellow), anti-Hts (red), and anti-LamC (red). Arrowheads indicate oocytes, which were also recognized by the presence of a karyosome. The frequency of egg chambers that lack an oocyte is quantified in C. (*Tnpo-SR^{RNAi}* egg chambers with less than 16 or more than 16 germ cells were excluded from this quantification.) (D-G) *Tnpo-SR^{GLC}* mutant mosaic germaria (D-D', F-F') labeled with anti-GFP (green; wild-type cells), anti-Hts and anti-LamC (red), and anti-Orb (blue; D-D') or anti-C(3)G (blue, F-F'). Quantification of the percentage of Orb-positive 16-cell cysts (germarium regions 2 and 3) and the number of C(3)G-positive cells are indicated in panels E and G, respectively. Red/blue channels only are shown in D' and F'. Yellow lines demarcate wild-type (solid) or mutant (dashed) cysts. Mosaics were analyzed 8 days after clone induction. All images of *Tnpo-SR^{GLC}* GSCs are from *Tnpo-SR^{KG}* females. Scale bar, 20 μm (A-B) and 10 μm (D-D', F-F'). Numbers in the bars represent the total number of egg chambers or germline cysts analyzed. ****p* < 0.001; Chi-square test.
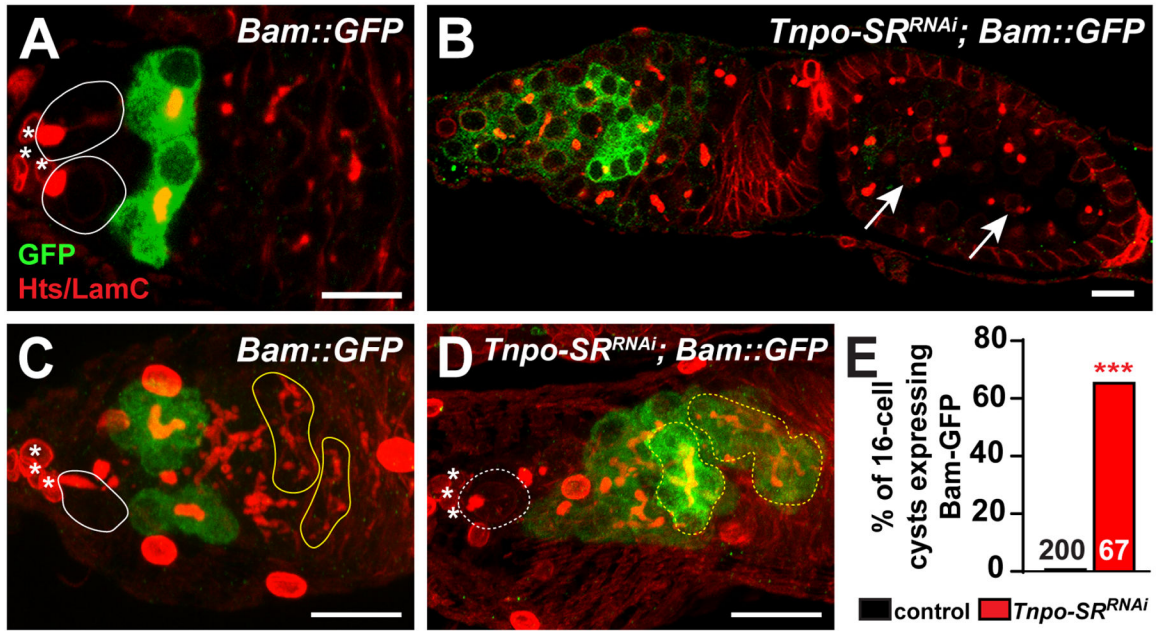
Figure 6. *Tnpo-SR*-depleted germ cells fail to suppress the differentiation factor Bam.
(A-D) Single z-plane images (A-B) or maximum intensity projections (C-D) of control
(A, C) or *nos-Gal4>Tnpo-SR^{RNAi}* (B, D) germaria expressing *Bam-sfGFP* labeled with
anti-GFP (for *Bam-sfGFP*, green), anti-Hts (red), and anti-LamC (red). Arrows indicate
germ cells in a tumorous egg chamber filled with single dot-like fusomes that do not express
Bam::GFP, resembling cystoblasts. Lines demarcate wild-type (solid) or mutant (dashed)
GSCs (white) and cystoblast/cysts (yellow); asterisks indicate cap cells. Scale bars, 10
μm. (E) Percentage of 16-cell cysts expressing *Bam-sfGFP* in control and *nos-Gal4>Tnpo-
SR^{RNAi}* germaria; numbers in bars indicate number of 16-cell cysts analyzed. ***$p < 0.001$,
Chi-square test.
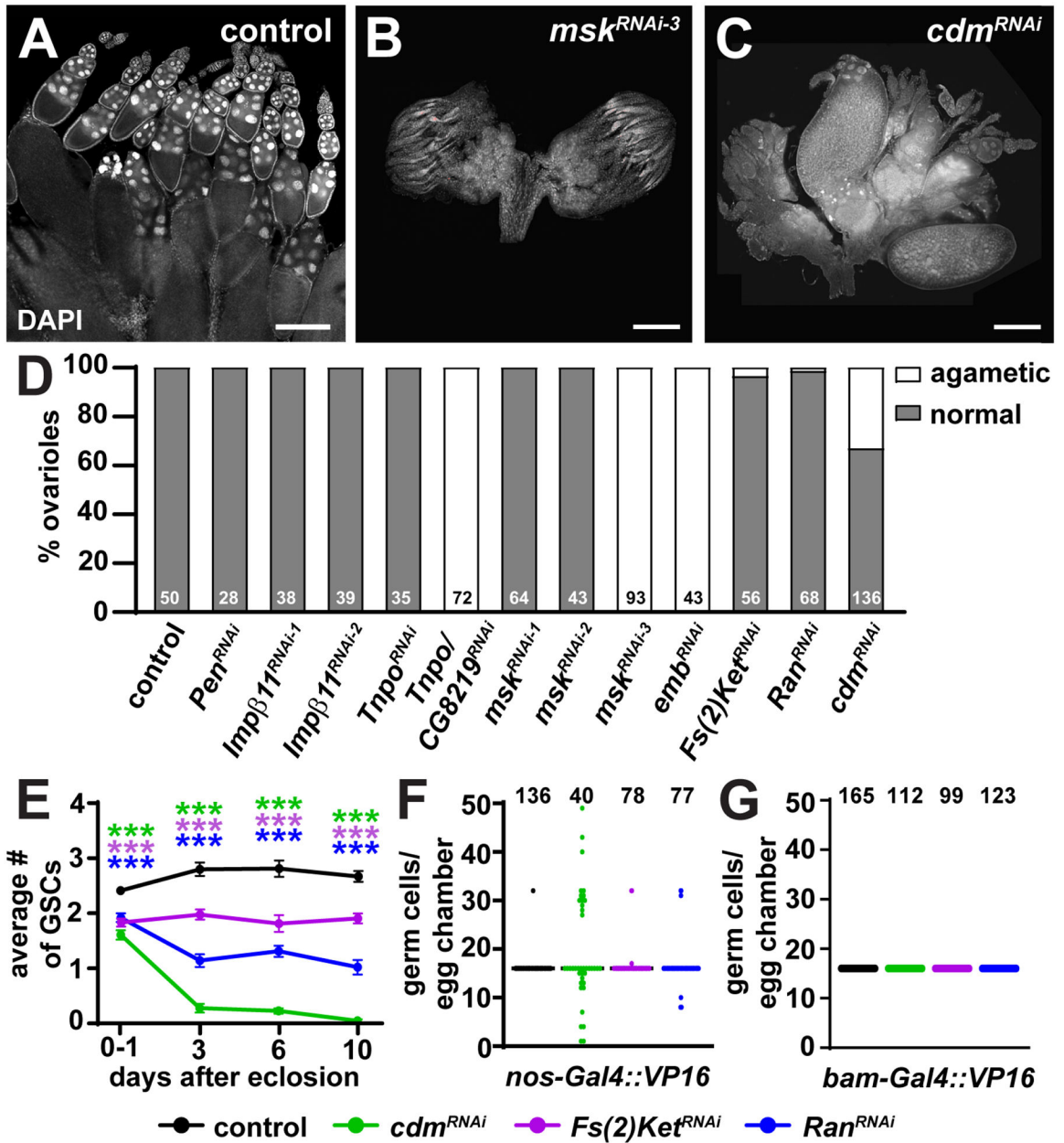
Figure 7. An RNAi screen identifies related roles for β-importin Cadmus and the GTP-binding protein Ran in GSC establishment and maintenance and germ cell mitoses.

(A-C) Maximum intensity projections of *nos-Gal4* control (A), *nos-Gal4>UAS- msk^RNAi-3* (B), or *nos-Gal4>UAS-cdm^RNAi* (C) ovaries labeled with DAPI (white; nuclei). Scale bar, 100 μm. (D) Frequencies of ovarioles containing agametic (white) egg chambers. (E) Average number of GSCs per germarium in *nos-Gal4* controls and *nos-Gal4>RNAi* mutants. More than 50 germaria per genotype at each timepoint were analyzed. Error bars represent s.e.m. (F-G) Ovarioles expressing *cdm^RNAi* (green), *Fs(2)Ket^RNAi* (purple), or *Ran^RNAi* (blue) driven with *nos-Gal4* (F) or *bam-Gal4* (G) were immunostained with anti-Hts, anti-LamC, and DAPI, and quantified for the number of germ cells per egg chamber. Each dot

represents one egg chamber. Numbers in bars (D) or above dots (F-G) represent the total number of egg chambers analyzed. ***$p < 0.001$; Student's two-tailed T-test.